Erschienen in: Natural Product Reports ; 38 (2021), 3. - S. 566-585
https://doi.org/10.1039/D0NP00056F

Chemistry of fungal meroterpenoid cyclases

Lena Barra[a] and Ikuro Abe *[ab]

Fungal meroterpenoid cyclases are a recently discovered emerging family of membrane-integrated, non-canonical terpene cyclases. They catalyze the conversion of hybrid isoprenic precursors towards complex scaffolds and are therefore of great importance in the structure diversification in meroterpenoid biosynthesis. The products of these pathways exhibit intriguing molecular scaffolds and highly potent bioactivities, making them privileged structures from Nature and attractive candidates for drug development or industrial applications. This review will provide a comprehensive and comparative view on fungal meroterpenoid cyclases, their intriguing chemistries and importance for the scaffold formation step towards polycyclic meroterpenoid natural products.

1 Introduction

Fungal meroterpenoids are a diverse family of hybrid natural products with potent bioactivities and intriguing structural architectures.[1–3] Several members are known as medicinal drugs, drug leads, or commercial insecticides. Pyripyropene A (**1**) is one of the few and most potent known selective inhibitors of the therapeutic target sterol *O*-acyltransferase 2 (SOAT-2) and therefore regarded as a promising drug candidate for the treatment of atherosclerosis and hypercholesterolemia (Fig. 1).[4–6] Additionally, **1** exhibits selective aphicidal activity whilst lacking mammalian toxicity.[7–9] Based on the core structure of **1**, the semisynthetic derivative afidopyropen (**2**) has been developed[10,11] and recently marketed as an eco-friendly, commercial insecticide.[12] Mycophenolic acid (**3**) in the form of the prodrug mycophenolate mofetil (**4**) is one of the most widely used immunosuppressive drugs for the treatment of organ transplant patients and inhibits inosine monophosphate dehydrogenase type 2 in *de novo* purine biosynthesis, leading to limited lymphocyte proliferation.[13–16] Subglutinol A (**5**) and derivatives have earned significant attention for their highly potent immunosuppressive properties, superior to cyclosporine and additionally lacking toxicity. These features make them highly attractive drug candidates for treating autoimmune

[a]*Graduate School of Pharmaceutical Sciences, The University of Tokyo, 7 3 1 Hongo, Bunkyo ku, Tokyo 113 0033, Japan. E mail: abei@mol.f.u tokyo.ac.jp*
[b]*Collaborative Research Institute for Innovative Microbiology, The University of Tokyo, Yayoi 1 1 1, Bunkyo ku, Tokyo 113 8657, Japan*

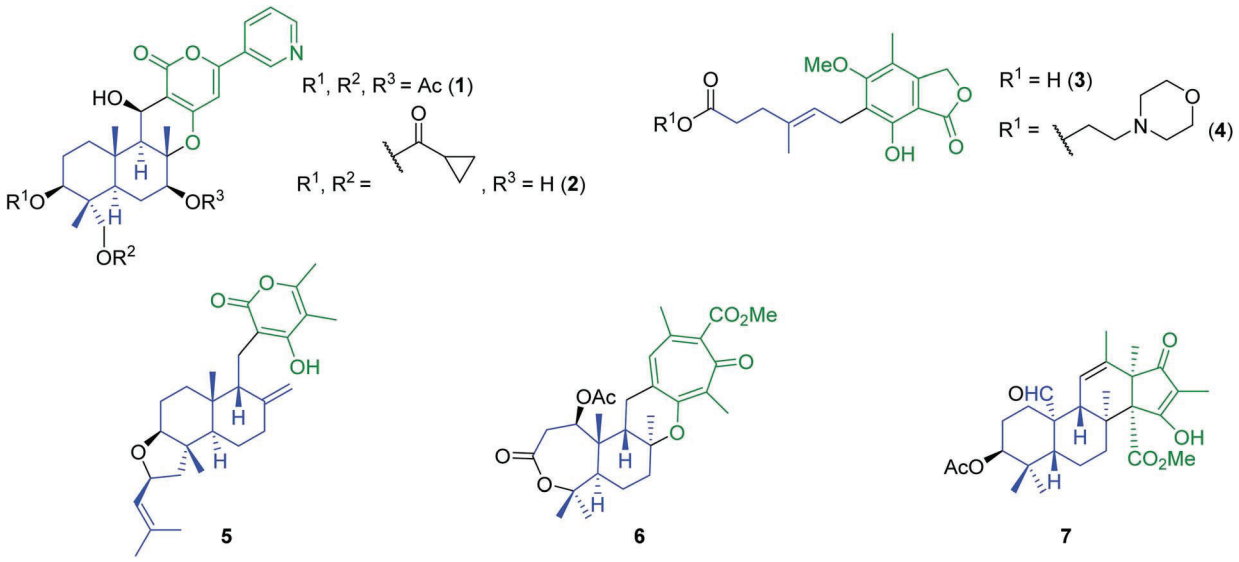

Fig. 1 Selected examples of fungal meroterpenoids and derivatives: pyripyropene A (1), afidopyropen (2), mycophenolic acid (3), mycophenolate mofetil (4), subglutinol A (5), tropolactone B (6), and andrastin A (7). The terpenoid portion is shown in blue, non-terpenoid in green.

diseases such as multiple sclerosis, type I diabetes mellitus, rheumatoid arthritis or systemic lupus erythematosus.[17 20]

Two examples of meroterpenoids with promising cytotoxic activities are tropolactone B (6) against human colon carcinoma[21] and the protein farnesyltransferase inhibitor andrastin A (7).[22,23]

The term "meroterpenoid", etymologically derived from the greek word "meros", meaning fragment or partial, refers to the

Lena Barra studied chemistry at the TU Braunschweig and obtained her master's degree in 2013. For her doctoral studies she joined the laboratory of Prof. Dr Jeroen S. Dickschat, working on mechanistic investigations in secondary metabolite biosynthetic pathways. After receiving her doctoral degree from the University of Bonn in 2018, she became a postdoctoral researcher in the work group of Prof. Dr Ikuro Abe at the University of Tokyo. Her research interest lies in the discovery of novel biosynthetic enzymes and how to exploit and engineer these biocatalysts as synthetic tools.

Ikuro Abe received his B.S. (1984) and Ph.D. (1989) from The University of Tokyo under the direction of Professors Ushio Sankawa and Yutaka Ebizuka, where he studied chemistry and biochemistry of natural products biosynthesis. After postdoctoral research with Professor Guy Ourisson at the CNRS Institut de Chimie des Substances Naturelles, and mostly with Professor Michel Rohmer at the Ecole Nationale Supérieure de Chimie de Mulhouse (1989–1991), he stayed in the United States to work with Professor Glenn D. Prestwich at the State University of New York at Stony Brook (1991–1996) and then at the University of Utah (1996–1998). In 1998, he moved back to Japan to join the faculty at University of Shizuoka (1998–2009), and then was appointed as Professor of Natural Products Chemistry at the Graduate School of Pharmaceutical Sciences, The University of Tokyo (2009–). His research interests mostly focus on exploring and engineering the natural products biosynthesis. He received The Japanese Society of Pharmacognosy Award (2017), Sumiki Umezawa Memorial Award (2017), The Pharmaceutical Society of Japan Award (2019), and Prizes for Science and Technology by the Minister of Education, Culture, Sports, Science and Technology, Japan (2019). He is a Fellow of The Royal Society of Chemistry (FRSC) and a former President of The Japanese Society of Pharmacognosy.

hybrid nature of these compounds, being composed of a terpenoid and a non-terpenoid portion (Fig. 1). In recent years, the growing knowledge about the genetic and molecular basis of meroterpenoid biosynthesis allowed to further specify and categorize meroterpenoids by their biosynthetic origins. Three major classes, differing in the non-terpenoid scaffold can be defined: the polyketide terpenoids (PK-T), the indole terpenoids (ID-T) and the shikimate-derived meroterpenoids.[1–3] These classes can be further subdivided by the origin of the terpenoid portion and biosynthetic pathways derived from the C_{15}-oligoprenyl diphosphate precursor farnesyl diphosphate (FPP) and the C_{20}-congener geranylgeranyl diphosphate (GGPP) towards polyketide sesquiterpenoids (PK-ST), polyketide diterpenoids (PK-DT) and indole diterpenoids (ID-DT) have been discovered from fungal sources (Table 1).

The isoprenoid portion of meroterpenoids can be acyclic as in the achiral meroterpenoid **3**, but in most cases complex (poly) cyclic structures bearing several stereocenters are present.

Table 1 Overview on reported and biochemically characterized fungal Pyr4-like meroterpenoid cyclases. The two Pyr4-like bacterial cyclases XiaE and DtmA1, as well as the atypical cyclases AscI and AtnI/NtnI are also given

Cyclase[a] (sequence similarity/identity (AA) to Pyr4)	Organism	Biosynthetic pathway	Bioactivity of pathway product	Type[b]
Pyr4 [27] (100%/100%)	*Aspergillus fumigatus* Af293	Pyripyropene A	Sterol *O* acyltransferase 2 (SOAT 2) inhibitor, atherosclerosis, hypercholesterolemia;[4–6] aphicidal[7–9]	PK ST
AusL[28,29] (67%/34%)	*Aspergillus nidulans*	Austinol	Unknown	PK ST
Trt1 [30–33] (58%/26%)	*Aspergillus terreus*	Terretonin	Mycotoxin[34]	PK ST
AdrI[35–37] (65%/29%)	*Penicillium chrysogenum* Wisconsin 54 1255	Andrastin A	Protein farnesyltransferase inhibitor, antitumor[22,23]	PK ST
PrhH[38] (69%/31%)	*Penicillium brasilianum* NBRC 6234	Paraherquonin/ berkeleydione	Metalloproteinase 3 and caspase 1 inhibitor, antitumor[39,40]	PK ST
NvfL[41,42] (71%/42%)	*Aspergillus novofumigatus*	Novofumigatonin	Unknown	PK ST
AndB[43–45] (69%/37%)	*Emericella variecolor* NBRC 32302	Anditomin/emeridone F	Cytotoxic,[46] antitumor	PK ST
CdmG[47] (82%/52%)	*Penicillium verruculosum* TPU1311	Chrodrimanins	Protein tyrosine phosphatase 1B inhibitor, type 2 diabetes, obesity[48]	PK ST
AscF[49,50] (58%/25%)	*Acremonium egyptiacum* F 1392	Ascochlorin	Antimicrobial,[51] anti inflammatory,[52] antiatherogenic,[53] cytotoxic[54]	PK ST
AscI[49] (atypical, 34%/8%)	*Acremonium egyptiacum* F 1392	Ascofuranone	Cytotoxic,[54] antimicrobial,[55] antiparasidic (*Trypanosoma brucei T. brucei*)[56]	PK ST
MacJ[57,58] (63%/29%)	*Penicillium terrestris* LM2	Macrophorin A	Immunosuppressive[59]	PK ST
OlcD[60] (68%/34%)	*Penicillium canescens* ATCC 10419	Deoxyoxalicin B	Insecticidal[61,62]	PK DT
Cle7 [63] (71%34%)	*Aspergillus versicolor* 0312	Chevalone E	Synergistic to doxorubicin, breast cancer[63]	PK DT
Sre3 [63] (67%/32%)	*Aspergillus felis* 0260	Sartorypyrone D	Synergistic to doxorubicin, breast cancer[63]	PK DT
SubB[64,65] (71%/49%)	*Metarhizium robertsii*	Subglutinol A	Immunosuppressive, no toxicity[17–20]	PK DT
AtnI/NtnI[66] (atypical, 18%/ 18%)	*Arthrinium* sp. NF2194, *Nectria* sp. Z14 w	Arthripenoids A F	Immunosuppressive[66]	PK DT
PaxB[67] (72%/44%)	*Penicillium paxilli*	Paxilline	Tremorgenic[68,69]	ID DT
NodB[70] (74%/47%)	*Hypoxylon pulicicidum*	Nodulisporic acids	Insecticidal[71]	ID DT
AtS5B1 [72] (73%/42%)	*Aspergillus flavus*	Emindole PB	Unknown	ID DT
AtS2B[72] (71%/35%)	*Aspergillus flavus*	Anominine[c] and 10,23 dihydro 24,25 dehydroaflavinine	Insecticidal[73] and insecticidal[74]	ID DT
AfB[72] (68%/32%)	*Aspergillus tubingensis*	Aflavinine	Insecticidal[75,76]	ID DT
XiaE[d,77–79] (bacterial, 52%/ 18%)	*Streptomyces* sp. SCSIO 02999, *Streptomyces* sp. HKI0576	Xiamycin A	Antiviral, anti HIV[80]	ID ST
DmtA1 [81] (bacterial, 51%/ 22%)	*Streptomyces youssoufiensis* OUC6819	Drimentine G	Cytotoxic,[82] antitumor	ID ST

[a] For homologous proteins with identical function, the first characterized member was selected. [b] PK ST polyketide sesquiterpenoid, PK DT polyketide diterpenoid, ID DT indole diterpenoid, ID ST indole sesquiterpenoid. [c] Initially named nominine, later renamed to anominine. [d] Named XiaH in ref. 77.

Compared to classical terpene cyclases, which activate and cyclase a purely terpenoic substrate in terpenoid biosynthesis,[24 26] specialized and distinct cyclases have been discovered for meroterpenoid biosynthetic pathways.

The first and thus far largest group of discovered meroterpenoid cyclases is a protein family of compact, membrane-integrated enzymes, catalyzing diverse carbocation-mediated cascade reaction on hybrid meroterpenoid precursors in PK-T and ID-T pathways. These homologous group of enzymes can be referred to as Pyr4-like cyclases, named after the first discovered representative. Besides the family of Pyr4-like enzymes, a few atypical meroterpenoid cyclases have been discovered in fungal pathways which resemble the mechanistic features of Pyr4-like cyclases but are phylogenetically distinct proteins and show no homology to Pyr4 (Table 1).

This review aims to provide a comparative and comprehensive overview on the chemistry of fungal meroterpenoid cyclases with a focus on the emerging family of Pyr4-like cyclases. The discovery and basic features of these enzymes will be introduced in chapter 2. Chapter 3 will give an overview on discovered cyclases and the importance of their pathways products. The general features, phylogenetic relations and distinctness to other cyclization strategies known from meroterpenoid pathways is discussed. Chapters 4–6 will describe the cyclization mechanism of each enzyme in detail and will highlight their importance in the structure diversification towards potent meroterpenoids. The concluding chapter 7 will give a brief summary and outlook on the future potential of these biocatalysts for biosynthetic engineering efforts.

2 The model meroterpenoid cyclase – Pyr4 (pyripyropene A)

The first meroterpenoid cyclase was discovered in 2010 in the biosynthetic gene cluster of pyripyropene A (**1**) from the fungus *Aspergillus fumigatus* Af293.[27] Detailed genetic and biochemical analysis of the gene cluster revealed a modular biosynthetic logic for meroterpenoid biosynthesis, comprised of four general steps (Scheme 1). The first step comprises assembly of the non-terpenoid portion by the action of an iterative type I polyketide synthase (Pyr2). Pyr2, in tandem with the CoA-ligase Pyr1, converts nicotinic acid (**8**) and malonyl-CoA (**9**) into 4-hydroxy-6-(3-pyridinyl)-2*H*-pyran-2-one (HPPO, **10**). Subsequently, a UbiA-type prenyltransferase (Pyr6) assembles the terpenoid and non-terpenoid building blocks by transferring FPP to **10**, generating farnesyl-HPPO (**11**). After formation of the hybrid precursor it was cryptic which enzyme was responsible for the obvious polyene cyclization event towards the polycyclic product **1** since no designated, canonical terpene cyclase was initially located in the gene cluster. The lack thereof prompted the researchers to investigate a protein of unknown function (Pyr4) comprised of only 246 amino acids and predicted as an integral membrane protein. Biochemical analysis revealed that Pyr4 works in tandem with a flavin-dependent monooxygenase (Pyr5) which activates the precursor by a stereoselective epoxidation of the terminal double bond to yield (10*S*)-epoxyfarnesyl-HPPO (**12**). Compound **12** is then converted by Pyr4 to deacetyl pyripyropene E (**13**). Mechanistically, the cyclization reaction can be explained by initial protonation of the epoxide functionality generating a reactive carbocation species and triggering the subsequent cascade reaction. Attack of the C6–C7 double bond generates the first 6-membered ring and a tertiary cation on C7, followed by subsequent attack of the C2–C3 π-bond to yield a tertiary cation at C3. The cyclization cascade is terminated by intramolecular nucleophilic attack of the phenolic hydroxyl group of the pyrone moiety (Scheme 1). To which extent the polyene cyclization truly occurs by step-wise nucleophilic additions generating distinct intermediary cationic species or an at least partly concerted mechanism prevails has not been determined yet.

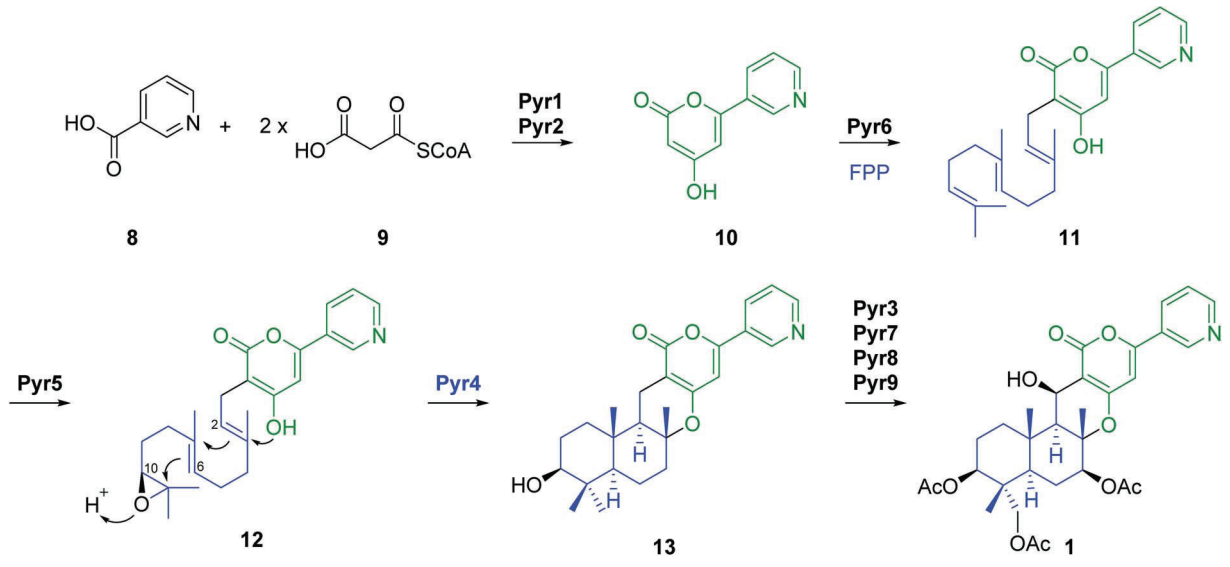

Scheme 1 Pathway towards pyripyropene (**1**) and depiction of meroterpenoid cyclase reaction catalyzed by Pyr4.

The stereochemical outcome of the polyene reaction is based on the substrate conformation, controlled by the active site cavity of the respective enzyme. For Pyr4 a chair–chair conformation can be envisioned to lead to the formation of **13** (Scheme 1 and Fig. 3A). The overall mechanism resembles that of type II terpene cyclases as found for 2,3-oxidosqualene-lanosterol synthase. However, Pyr4 shows no sequence homology and also lacks conserved motifs known from other canonical terpene cyclases.[24,25] The fourth general step in meroterpenoid assembly lines comprises the tailoring of the generated core scaffold. In pyripyropene A biosynthesis, two P450 monooxygenases (Pyr3 and Pyr9) and the acetyltransferases Pyr7 and Pyr8 generate the final product from deacetyl pyripyropene E (**13**) (Scheme 1).

3 Reported meroterpenoid cyclases – overview and general features

The elucidation of the genetic basis of pyripyropene A (**1**) biosynthesis with the discovery of the first membrane bound meroterpenoid cyclase Pyr4 facilitated the characterization of several homologous proteins in fungal polyketide and indole meroterpenoid pathways. Table 1 gives an overview on biochemically characterized Pyr4-like meroterpenoid cyclases (state July 2020), their biological origin and reported bioactivities of the respective pathway products. Besides fungal Pyr4-like cyclases, two homologous enzymes have also been identified from bacteria: XiaE from the pathway towards the indole sesquiterpenoid (ID-ST) xiamycin A[77 79] and DmtA1 involved in the diketopiperazine-terpene biosynthetic machinery for drimentines.[81] Furthermore, two atypical cyclases have been discovered in fungal biosynthetic pathways towards ascofuranone (AscI)[49] and arthripenoids (AtnI/NtnI). AscI and AtnI/NtnI exhibit no homology to the family of Pyr4-like enzymes but resemble the observed mechanism for activation and cyclization of hybrid substrates.[66]

Besides these meroterpenoid cyclases, a few non-canonical terpene cyclases have been identified in fungal meroterpenoid pathways. In these instances, cyclization of the terpenoid precursor occurs prior to the fusion of terpenoid and non-terpenoid portion. One example is the membrane-bound, UbiA-like terpene cyclase Af520 from the fumagillin pathway of *Aspergillus fumigatus*. Af520 converts FPP into β-*trans*-bergamotene and the cyclization mechanism is proposed to proceed *via* pyrophosphate abstraction similar to type I terpene cyclases.[84] A second example is AsR6, discovered in the biosynthetic gene cluster towards xenovulene A from *Acremonium strictum* IMI 501407. AsR6 was shown to be a Mg^{2+}-dependent humulene synthase with no homology to other known terpene cyclases and a downstream operating Hetero Diels-Alderase (AsR5) connects the monocyclic terpene with the polyketide scaffold.[85] Furthermore, a P450 monooxygenase-dependent cyclization strategy was discovered in the biosynthetic pathway towards viridicatumtoxin from *Penicillium aethiopicum*.[86] For a detailed discussion of these non-canonical terpene cyclases the reader is referred to a recently published, excellent review from Rudolf *et al.*[87] Meroterpenoid biosynthesis in *Streptomyces* bacteria has recently been reviewed by George *et al.*[88]

Pyr4-like cyclases are of compact size with a molecular weight of around 25 kDa and predicted as integral membrane proteins with seven transmembrane helices. Multiple protein sequence alignment shows the occurrence of several highly conserved amino acid residues (Fig. 2). Mutational studies on

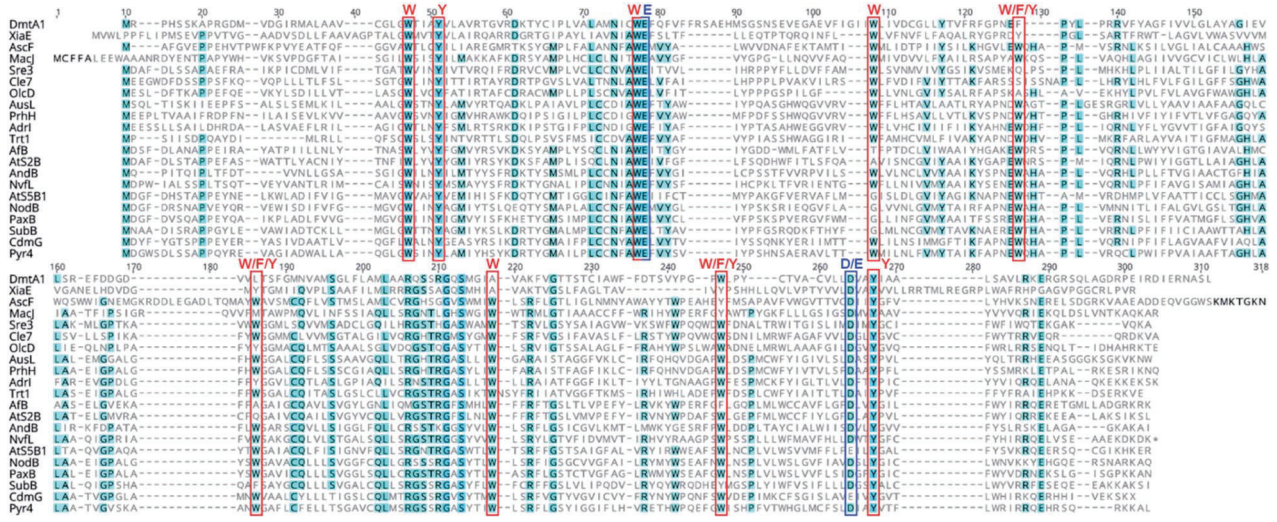

Fig. 2 Multiple sequence alignment of Pyr4-like meroterpenoid cyclases constructed with MUSCLE. Conserved acidic residues proposed to function in epoxide opening are highlighted in blue, aromatic amino acids proposed to stabilize cationic intermediates in red. NCBI protein accession numbers: XiaE (CCH63731), DmtA1 (AVP32200), AscF (ASCF_ACREG), MacJ (AVK70105), Sre3 (BBG67005), Cle7 (BBG28477), OlcD (EPS35035), AusL (XP_682526), PrhH (PRHH_PENBI), Adrl (ADRI_PENRO), Trt1 (XP_001209379), AfB (XP_002380346), AtS2B (OJI86757), AndB (ANDB_EMEVA), NvfL (XP_024677071), AtS5B1 (OJI82697), NodB (NODB_HYPPI), PaxB (PAXB_PENPX), SubB (EXU95682), CdmG (CDMG_TALVE), Pyr4 (XP_751270).

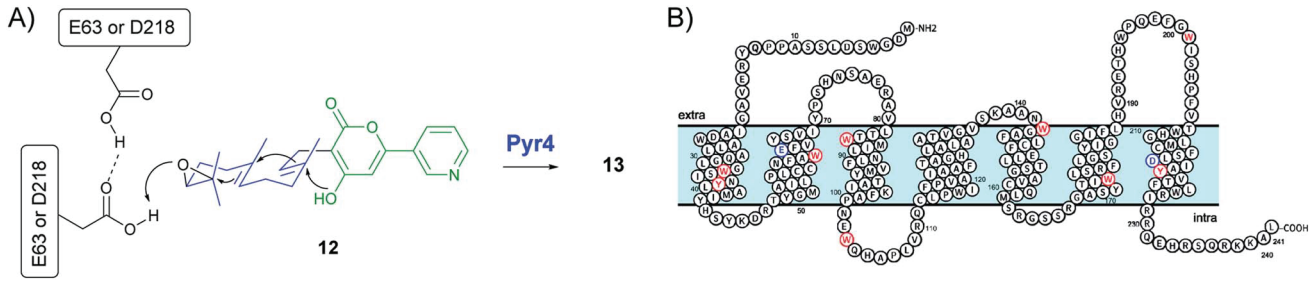

Fig. 3 (A) Proposed mechanistic functions of conserved amino acid residues E63 and D218 in Pyr4-mediated cyclization reaction. (B) Hydropathy plot model of Pyr4 using PROTTER.[83] Conserved acidic residues proposed to function in epoxide opening are highlighted in blue, aromatic amino acids proposed to stabilize cationic intermediates in red.

the model cyclase Pyr4 revealed that the two conserved acidic residues E63 and D218 (Pyr4 numbering) are essential for enzyme function and proposed to act as the acidic catalytic site responsible for the initiation of polyene cyclization by epoxide opening (Fig. 2 and 3A, highlighted in blue).[27] Mutational studies on the respective residues in the bacterial enzyme DmtA1 (51%/25% sequence similarity/identity (AA) to Pyr4) further supported these findings.[81] Based on the hydropathy plot protein modeling,[83] these conserved residues are located in the transmembrane region, suggesting a transmembrane localization of the enzyme active site (Fig. 3B, highlighted in blue).[27,81] Furthermore, the sequence alignment indicates the

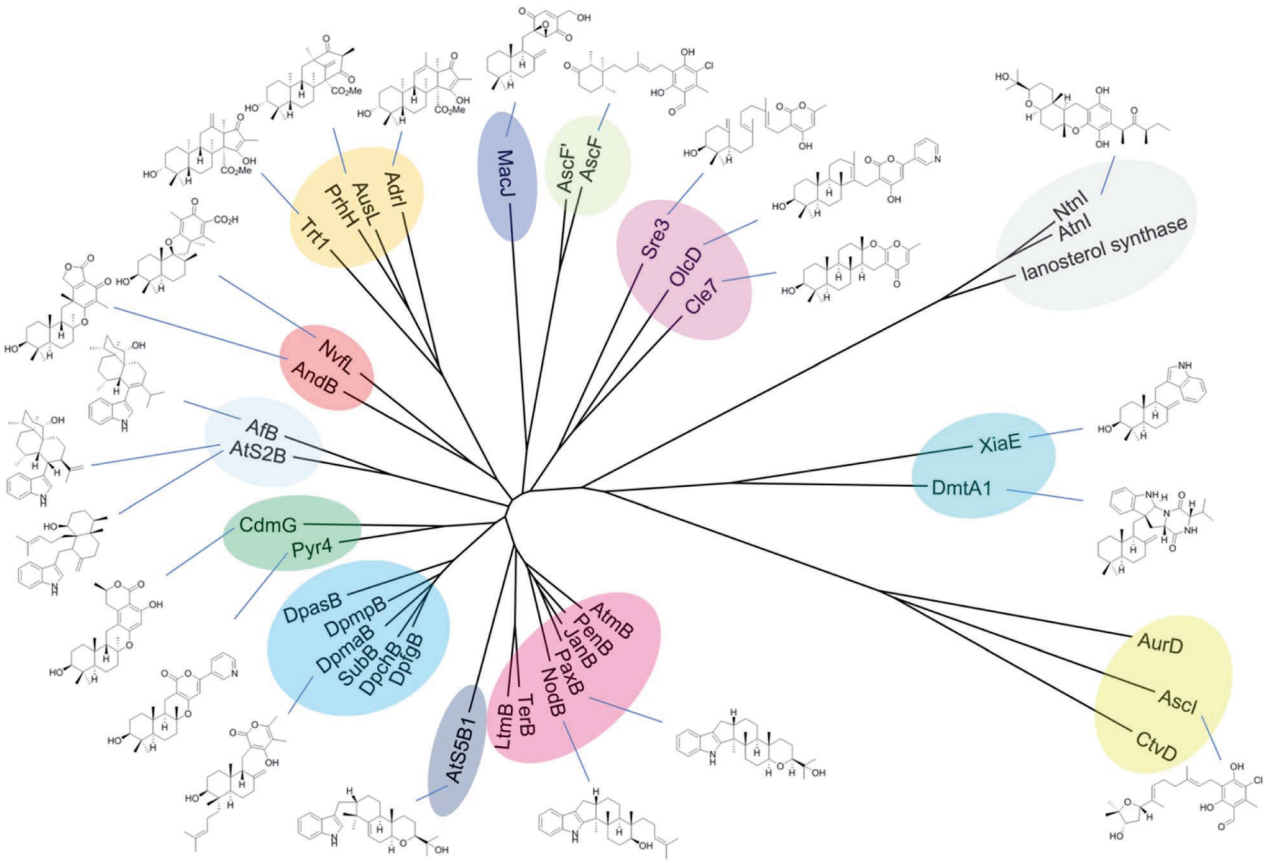

Fig. 4 Phylogenetic analysis of biochemically characterized fungal Pyr4-like meroterpenoid cyclases, the bacterial homologs XiaE and DmtA1, and the two atypical cyclases AscI and NtnI/AtnI constructed using MUSCLE alignment and neighbour-joining algorithm. The structures of the respective enzyme products are given. NCBI protein accession numbers: Pyr4 (XP 751270), Trt1 (XP 001209379), AusL (XP 682526), AdrI (ADRI PENRO), PrhH (PRHH PENBI), NvfL (XP 024677071), AndB (ANDB EMEVA), CdmG (CDMG TALVE), AscF (ASCF ACREG), AscF′ (BAZ95876), AscI (BBF25321), AurD (AURD CALAK), CtvD (CTVD ASPTN), MacJ (AVK70105), OlcD (EPS35035), Cle7 (BBG28477), Sre3 (BBG67005), SubB (EXU95682), DpmpB (MPH 09195), DpfgB (EYB27998), DpmaB (KFG81920), DpchB (CH63R 05476), DpasB (n.a.),[65] NtnI (MH183002), AtnI (MH183015), lanosterol synthase (XP 033416225), PaxB (PAXB PENPX), NodB (NODB HYPPI), AtmB (XP 025521422), LtmB (LTMB EPIFI), TerB (BAM84047), PenB (PENB PENCR), JanB (JANB PENJA), AtS5B1 (OJI82697), AtS2B (OJI86757), AfB (XP 002380346), XiaE (CCH63731), DmtA1 (AVP32200).

presence of several highly conserved aromatic amino acids (Fig. 2 and 3B, highlighted in red). Aromatic amino acids are electron-rich centers and therefore able to stabilize positive charges by cation–π interactions. For the well studied 2,3-oxidosqualene-lanosterol synthase and squalene-hopene cyclase repeated conserved QW-motifs are found. These amino acid residues line the active site cavity and are proposed to be responsible for the stabilization of concomitantly generated cationic centers during the polyene cyclization cascade reaction.[24,89] A similar function seems likely for the conserved aromatic amino acids in meroterpenoid cyclases which also seem to be dominantly located in the putative active site region in the transmembrane. Mutations on several conserved aromatic residues in DmtA1 were reported to abolish enzyme function, further supporting the importance of these residues for proper enzyme function.[81] However, the lack of protein structural data limits the understanding of the catalytic mechanism of the Pyr4-like enzyme family.

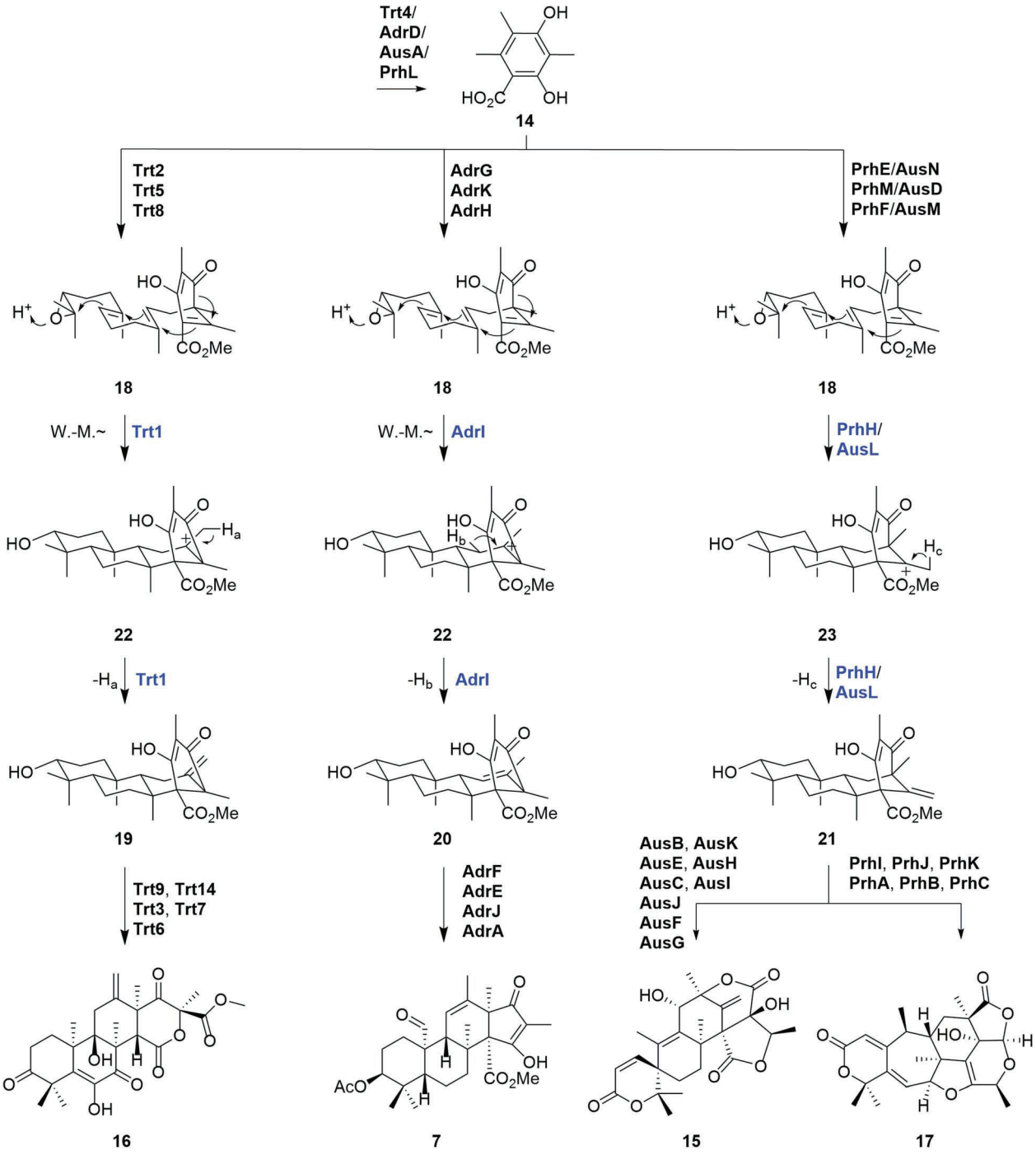

Scheme 2 Pathways towards DMOA-meroterpenoids terretonin (16), andrastin A (7), austinol (15), and paraherquonin (17) and detailed depiction of meroterpenoid cyclase reactions catalyzed by Trt1, AdrI, AusL and PrhH.

A phylogenetic analysis of reported fungal and bacterial Pyr4-like meroterpenoid cyclases and the two atypical cyclases AscI and AtnI/NtnI is provided in Fig. 4. The subsequent chapters will discuss the biosynthetic function and proposed cyclization mechanism of each cyclase in detail and will refer to phylogenetic relations.

4 Meroterpenoid cyclases in fungal PK-ST pathways

4.1 Four related meroterpenoid cyclases from DMOA pathways – AusL (austinol), Trt1 (terretonin), AdrI (andrastin A), and PrhH (paraherquonin)

A large group of fungal meroterpenoids contains the polyketide 3,5-dimethylorsellinic acid (DMOA, **14**) as the non-terpenoid building block[1–3] and the second discovered Pyr4-like meroterpenoid cyclase was AusL from the biosynthetic gene cluster of the DMOA-derived meroterpenoid austinol (**15**) from *Aspergillus nidulans* (Scheme 2).[28,29] Subsequent identification of pathways towards the mycotoxin terretonin (**16**) from *Aspergillus terreus*,[30–34] the protein farnesyltransferase inhibitor andrastin A (**7**) from *Penicillium chrysogenum* Wisconsin 54-1255,[22,23,35–37] and paraherquonin (**17**) from *Aspergillus brasilianum*[38] revealed a closely related biogenesis.

Following the conserved four-step assembly logic as for the pyripyropene (**1**) cluster, the first step comprises the formation of the non-terpenoid portion. DMOA (**14**) is generated by the action of homologous iterative type I polyketide synthases Trt4, AusA, AdrD, and PrhL in the respective cluster. Subsequent regio- and stereospecific dearomative farnesylation by a prenyl transferase (Trt2, AdrG, AusN, PrhE), additional methylation of the carboxylic acid function (Trt5, AdrK, AusD, PrhM), and stereospecific epoxidation by an FAD-dependent epoxidase (Trt8, AdrH, AusM, PrhF) generates the (10*R*)-epoxyfarnesyl intermediate **18**. The action of the respective terpene cyclase marks the branching point in each pathway as they catalyze differing transformations of the common substrate **18**. Whereas Trt1 catalyzes the formation of preterretonin A (**19**), AdrI produces andrastin E (**20**) and AusL (and PrhH) protoaustinoid A (**21**) (Scheme 2). Notably, the methylation of the carboxylic acid function of **18** is essential for the terpene cyclization reaction, as the demethylated substrate was not converted by any of the cyclases, based on *in vivo* results.

The proposed cyclization mechanism for Trt1 requires the substrate **18** to be prefolded in a chair–chair–chair conformation from which after acid-catalyzed epoxide opening the polyene cyclization occurs. The third ring-closing step involves C–C bond formation between the polyketide system and the farnesyl portion followed by a Wagner–Meerwein rearrangement to intermediary cation **22**. The terminating step in Trt1 catalysis comprises selective deprotonation of H_a from the adjacent methyl group resulting in the formation of a 6–6–6–5 ring system with an exocyclic double bond. Similar to Trt1, AdrI also catalyzes cyclization of **18** *via* the proposed intermediate **22**. However, the terminating step differs with respect to the deprotonation side as H_b is removed, leading to the cyclohexene moiety in andrastin E (**20**). AusL on the other hand catalyzes a chair–chair–chair conformational controlled cyclization to intermediary cation **23** which upon deprotonation of H_c yields the bridged [3.3.1] ring system of the protoaustinoid scaffold bearing a semicyclic olefin (**21**). The homologous protein PrhH catalyzes the same reaction as AusL and a downstream operating dioxygenase (PrhA)[38] diverges both pathways, leading to formation of paraherquonin (**17**) as the final product (Scheme 2).

Consistent with the obvious similarities in substrate and product specificity, the phylogenetic analysis of Trt1, AdrI, AusL, and PrhH reveals a close relation, as they are located on the same branch and form a specific clade (Fig. 4).

4.2 Spiro-ring formation – NvfL (novofumigatonin)

The meroterpenoid cyclase NvfL is found in the biosynthetic pathway towards the heavily oxygenated DMOA-derived novofumigatonin (**24**) and utilizes substrate **25** which is also derived

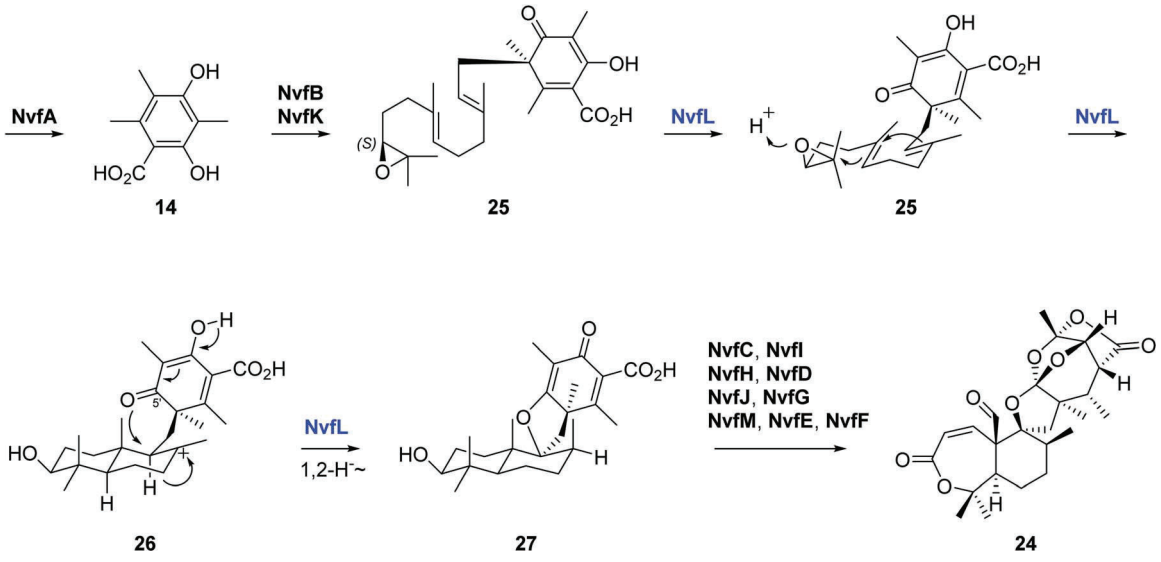

Scheme 3 Pathway towards novofumigatonin **24** and detailed depiction of meroterpenoid cyclase reaction catalyzed by NvfL.

from DMOA (**14**) and FPP but exhibits a carboxylic acid function instead of the methyl ester of **18** in priorly discussed DMOA-based pathways (Schemes 2 and 3).[41,42] Compared to **18**, **25** exhibits the opposite stereochemistry for the epoxide functionality with (10*S*)-configuration. NvfL was found to convert **25** *via* the proposed intermediate **26** into asnovolin H (**27**). The cyclization reaction can be envisioned from a prefolded substrate in chair–chair conformation from which after epoxide opening the bicyclic intermediary tertiary cation **26** is generated after sequential attack of the C6–C7 and C2–C3 double bonds. Instead of subsequent bond formation to the polyketide moiety, a 1,2-hydride shift precedes followed by terminating cation quenching from the oxygen in 5′-position of the polyketide portion leading to the formation of a spiro center. In *in vivo* experiments using the heterologous host *A. oryzae* it was shown that NvfL only accepts the free acid **25**, but not the methyl ester analogue **18**. This is interesting to note, since the methylation of the carboxylic acid group occurs after cyclization in the novofumigatonin (**24**) pathway and is discussed to inhibit spontaneous decarboxylation reactions.[3,42]

The phylogenetic analysis of NvfL reveals only a distant relation to the DMOA-methyl ester-accepting group of enzymes (Trt1, AdrI, AusL, PrhH) but a close relation to the cyclase AndB (Fig. 4).

4.3 Chair–Boat conformational control – AndB (anditomin) and CdmG (chrodrimanin B)

All discussed meroterpenoid cyclases trigger polyene cyclization from the thermodynamically favored all-chair conformation.

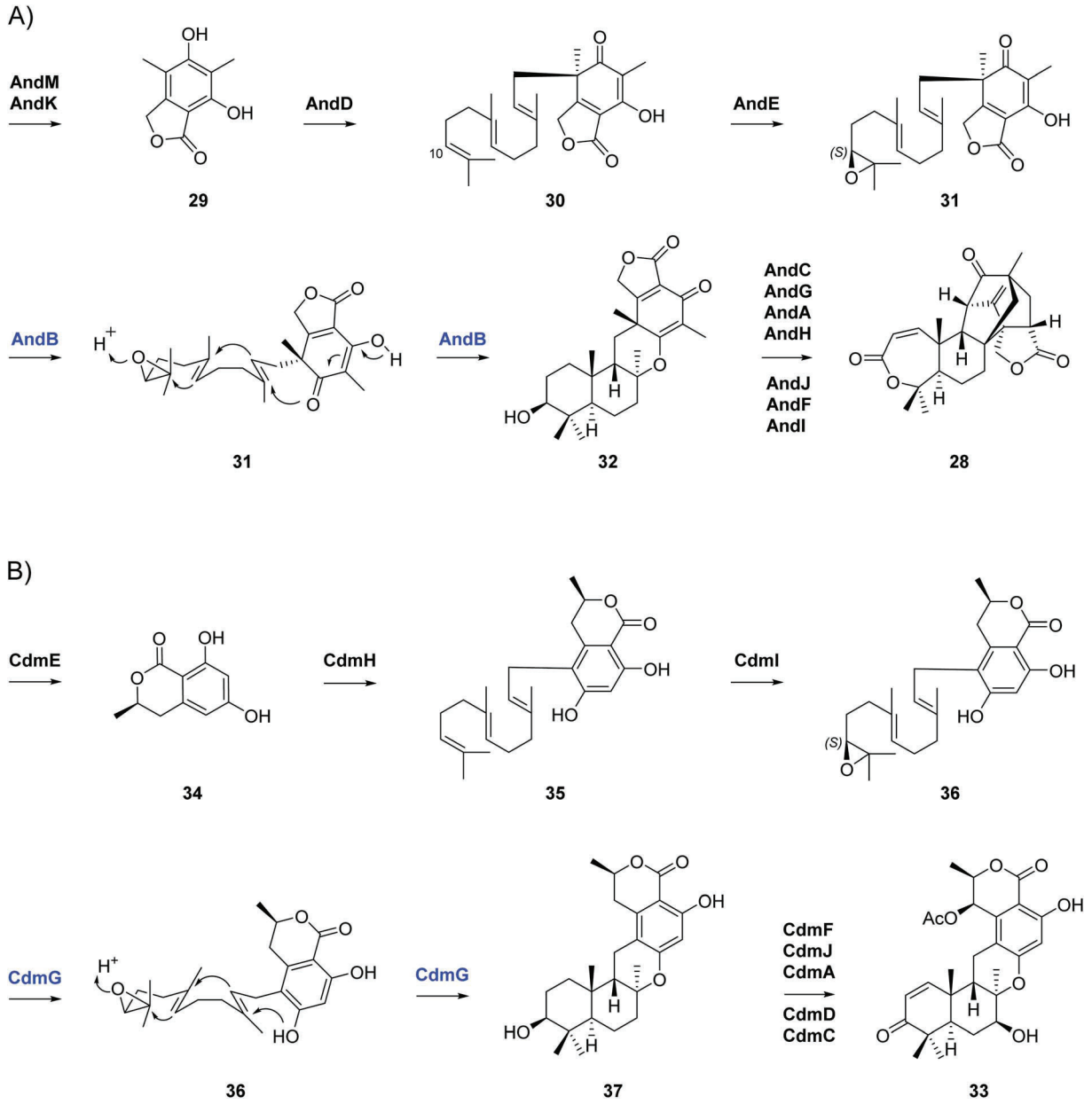

Scheme 4 (A) Pathway towards anditomin (**28**) and detailed depiction of meroterpenoid cyclase reaction catalyzed by AndB. (B) Pathway towards chrodrimanin B (**33**) and detailed depiction of meroterpenoid cyclase reaction catalyzed by CdmG.

The first cyclase found to catalyze with chair–boat–chair stereocontrol was AndB, discovered in the anditomin (**28**) biosynthetic gene cluster from *Emericella variecolor* NBRC 32302 (Scheme 4A).[43 45]

The substrate of AndB is assembled by an iterative type I PKS (AndM), generating DMOA (**14**) which upon the action of a chimeric P450/dehydratase enzyme (AndK) is oxidized and lactonized to 5,7-dihydroxy-4,6-dimethylphthalide (DHDMP, **29**). The prenyltransferase AndD subsequently catalyzes stereospecific farnesylation of DHDMP (**29**) giving rise to farnesyl-DHDMP (**30**). As found in the novofumigatonin (**24**) and pyripyropene (**1**) pathway, an FAD-dependent monooxygenase (AndE) introduces the epoxide functionality from the 10*Si*,11*Re*-face and generates (10*S*)-epoxyfarnesyl-DHDMP (**31**). The designated Pyr4-like terpene cyclase in the anditomin (**28**) cluster AndB then catalyzes formation of preandiloid A (**32**). The observed stereochemical outcome of the cyclization can be explained by a chair–boat conformation from which after initial epoxide opening the polyene cyclization occurs and is terminated by a C–O bond formation to the phenolic hydroxyl group of the polyketide portion (Scheme 4A).

The only other reported meroterpenoid cyclase which catalyzes product formation from a chair–boat conformation is CdmG, found in the biosynthetic gene cluster towards chrodrimanins from *Penicillium verruculosum* (Scheme 4B).[47] Chrodrimanin B (**33**) has strong inhibitory activities against protein tyrosine phosphatase 1B (PTP1B) and is discussed as a potential drug candidate for the treatment of type 2 diabetes and obesity.[48]

The pathway towards **33** comprises the formation of 6-hydroxymellein (**34**) by the PKS CdmE which upon farnesylation by CdmH to **35** and subsequent (*S*)-selective epoxidation yields the cyclase substrate **36**. Apparent from the *trans*-configured B/C-ring system in the terpene cyclase product 3-hydroxypentacecilide A (**37**), a chair–boat conformation must control the epoxide opening-induced cyclization cascade catalyzed by CdmG (Scheme 4B).

Although AndB and CdmG both catalyze product formation *via* chair–boat substrate conformation, they are not located on a shared branch in the phylogenetic analysis. AndB shows a closer relation to NvfL which might be reflected by the shared utilization of a DMOA-derived substrate (compound **25** for NvfL and **31** for AndB). CdmG on the other hand seems to be closely related to Pyr4 and both substrates (compound **12** for Pyr4 and **36** for CdmG) exhibit an α-pyrone substructure (Fig. 4).

4.4 Early abortion of cyclization and elaborate rearrangement – AscF (ascochlorin)

The majority of known Pyr4-like meroterpenoid cyclases catalyze polyene cyclizations towards tetracyclic ring systems. A cyclase which was found to produce an early cyclization abortion product instead is AscF from the pathway towards the antimicrobial,[51] anti-inflammatory,[52] antiatherogenic,[53] and cytotoxic[54] agent ascochlorin (**38**) from *Acremonium egyptiacum* F-1392 (synonym: *Acremonium sclerotigenum*)[49] and *Fusarium* sp.[50] (AscF′ in Fig. 4) (Scheme 5). AscF utilizes the orsellinic acid (**39**)-derived substrate ilicicolin A epoxide (**42**), arising from farnesylation (AscA), reduction (AscB), chlorination (AscD), and subsequent epoxidation (AscE). It is interesting to note that instead of a flavin-dependent monooxygenase a soluble P450 monooxygenase/P450 reductase fusion protein (AscE) was found to be responsible for the activation of the precursor by stereospecific epoxidation to form the (10*S*)-configured epoxide

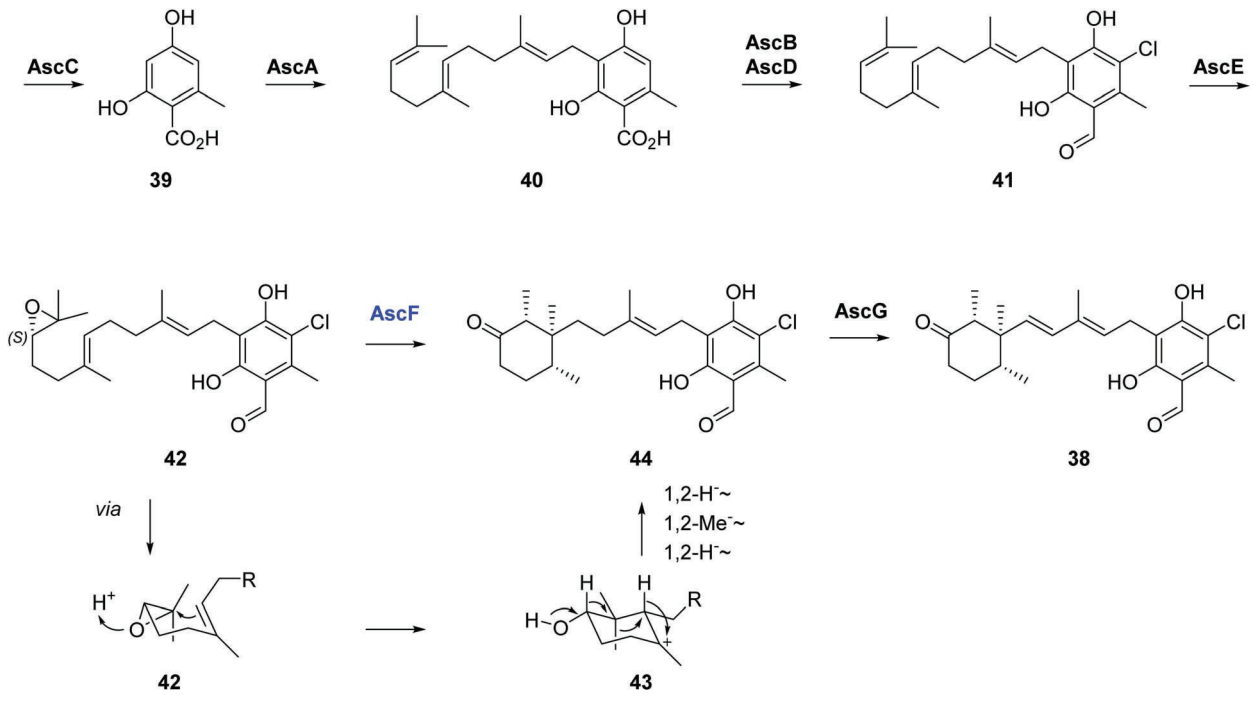

Scheme 5 Pathway towards ascochlorin (**38**) and detailed depiction of meroterpenoid cyclase reaction catalyzed by AscF.

42. The cyclization reaction catalyzed by AscF converts **42** *via* intermediary cation **43** into ilicicolin C (**44**) and is thus able to abort the cascade reaction after the first cyclization process. The reaction mechanism is suggested to yield intermediary cation **43** after initial epoxide opening and attack of the C6–C7 double bond, followed by sequential suprafacial 1,2-hydride shift, 1,2-methyl migration, 1,2-hydride shift and final deprotonation of the hydroxyl group (Scheme 5).

In agreement with the observed unusual cyclization reaction of AscF, this cyclase seems to be distinct to other reported Pyr4-like meroterpenoid cyclases. In the phylogenetic tree, AscF is located on a separate branch and is not clustered with any other cyclase (Fig. 4). This finding is also supported by a slightly longer protein sequence of AscF (267 AA), giving rise to an inserted sequence of eleven amino acid residues around position 155 and a 14 amino acid residues longer C-terminal region (Fig. 2). However, AscF shares the commonly observed sequence motifs for Pyr4-like cyclases and is also predicted to exhibit seven transmembrane helices (Fig. 2).

4.5 The atypical cyclase AscI (ascofuranone)

The ascochlorin (**38**) producing strain *A. egyptiacum* additionally contains the biosynthetic genes towards the structurally related compound ascofuranone (**45**) (Scheme 6).[49] Ascofuranone is a highly potent compound with diverse physiological activities such as antitumor,[54] anti-microbial,[55] and antiparasidic activities.[56] Most notably, the strong inhibitory activity against cyanide-insensitive alternative oxidases makes **45** a promising drug-candidate for the treatment of African trypanosomiasis (African sleeping sickness) caused by the trypanosome alternative oxidase-dependent protozoan parasite *Trypanosoma brucei*.[50,56] The discovery of the biosynthetic gene cluster for **45** paved the way to develop a cost-effective production by biotechnological methods.

The biosynthesis of **45** branches from the ascochlorin (**38**) pathway by the action of the P450 monooxygenase AscH which catalyzes an (*R*)-selective hydroxylation at C8 on shared intermediate **42** to generate **46** (Scheme 6). The cyclic ether formation, which can be regarded as a type II terpene cyclization reaction is catalyzed by AscI and can be explained by protonation of the epoxide and subsequent attack of the hydroxyl group to form ascofuranol (**47**). AscI is predicted to comprise eight transmembrane helices and shows no homology to Pyr4-like terpene cyclases. However, a sequence similarity/identity (AA) of 52%/22% and 46%/20% to the regioselective hydrolases CtvD in citreoviridin[90] and AurD in aurovertin biosynthesis[91] was found (Fig. 4). These enzymes catalyze the formation of 3,4-dihydroxy-tetrahydrofuran structures from the respective bisepoxides.

Notably, the biosynthetic gene cluster for ascofuranone (**45**) is distributed on two different loci in the genome (*asc-1* and *asc-2*). Whereas *asc-1* harbors all biosynthetic genes for ascochlorin (**38**) assembly, *asc-2* contains the genes *ascH*, *ascI* and *ascJ*.[50]

4.6 Cyclization initiated by double bond protonation – MacJ (macrophorins)

All characterized meroterpenoid pathways share the common oxidative cyclization sequence by employing an epoxidase for substrate activation and subsequent cyclization by a membrane-bound terpene cyclase. The only known fungal Pyr4-like cyclase which differs from this commonly observed strategy is MacJ from the biosynthetic pathway towards immunosuppressive[59] macrophorins A–D (**48–51**) from *Penicillium terrestris* LM2 (Scheme 7B).[58] Macrophorins are structurally related to their linear congeners, the group of yanuthones (**52–55**), which exhibit antibacterial properties (Scheme 7A).[92] The discovery of the biosynthetic pathway towards yanuthone D (**55**) in *Aspergillus niger* revealed that the non-terpenoid unit is assembled by a PKS (YanA) generating 6-methyl salicylic acid (6-MSA, **56**) which after further tailoring (YanB, YanC, YanD, YanE) to **57** is farnesylated by YanG to **58**. Subsequently, the building block is further decorated by hydroxylation, transfer of a 3-hydroxy-3-methylglutaryl group (YanI) and oxidation of the hydroxyl function by YanF to yield the quinoid-like yanuthone D (**55**) (Scheme 7A).[57]

In subsequent studies it was found that several biosynthetic gene clusters homologous to the *mac*-cluster exist which contain an additional Pyr4-like meroterpenoid cyclase,

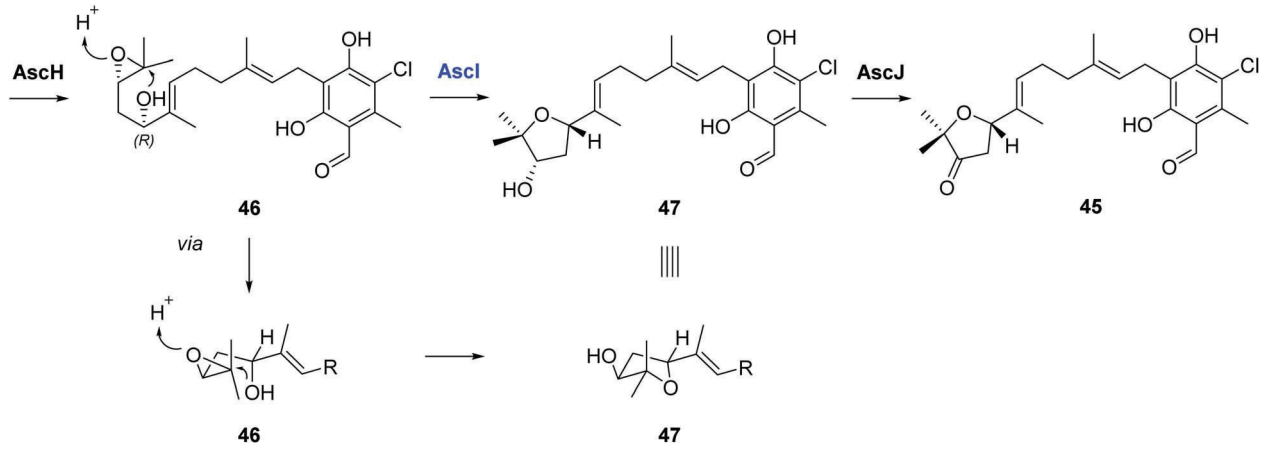

Scheme 6 Pathway towards ascofuranone (**45**) and detailed depiction of meroterpenoid cyclase reaction catalyzed by AscI.

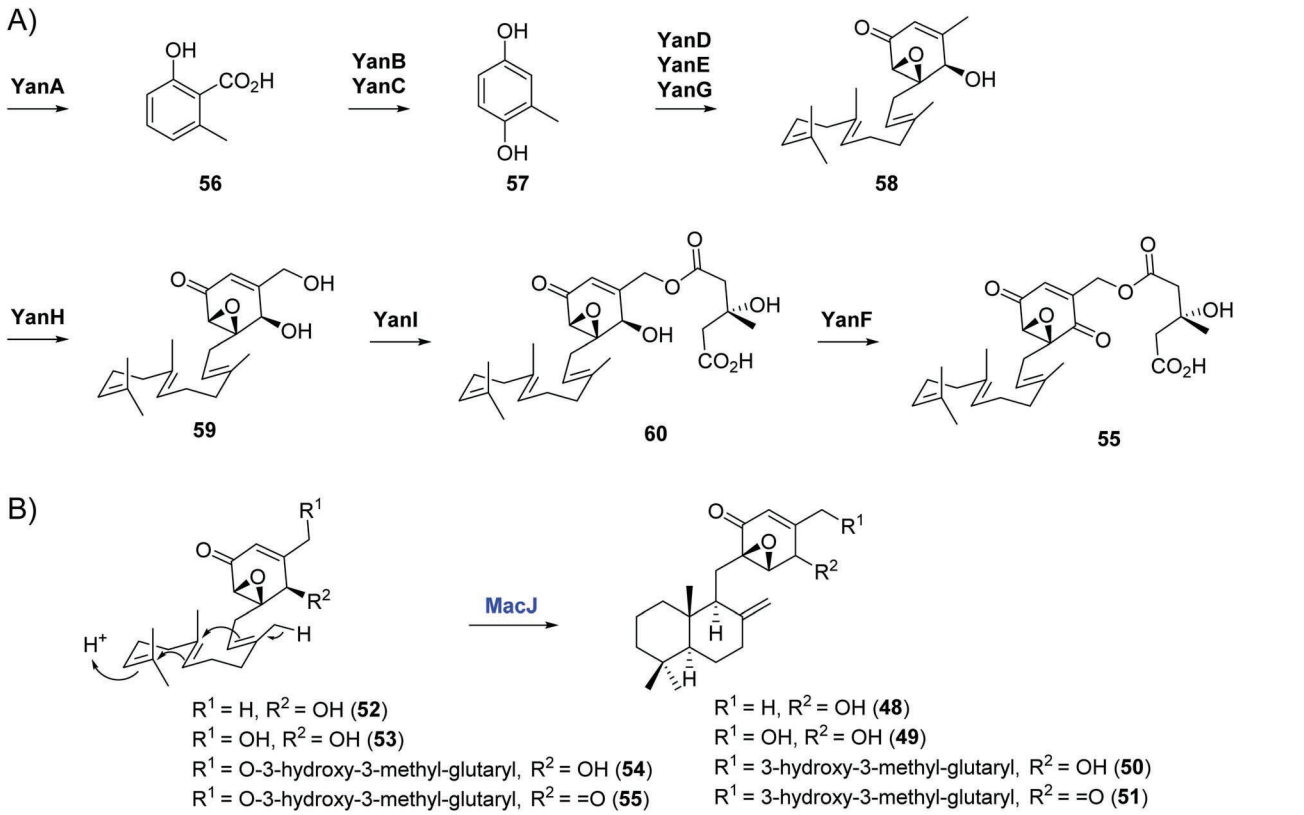

Scheme 7 (A) Pathway towards linear epoxycyclohexenone yanuthones (**55**). (B) Late-stage cyclization catalyzed by MacJ towards macrophorins A–D (**48–51**).

homologous to Pyr4.[58] In *in vivo* and *in vitro* studies using *Saccharomyces cerevisiae* as expression host, it was shown that MacJ is able to convert the isoprenic precursors **52–55** to their respective cyclized products **48–51** without the involvement of a prior epoxidation step. Therefore, MacJ is able to directly protonate the C10–C11 double bond in the farnesyl chain and catalyze a chair–chair-guided cyclization which is terminated by deprotonation to form the exomethylene group present in the resulting drimane scaffolds (Scheme 7B). Notably, MacJ exhibits high substrate promiscuity with respect to differing substitution patterns in the polyketide moiety and is therefore an attractive target for combinatorial biosynthesis.

The only other Pyr4-like cyclase which initiates polyene cyclization by direct double bond protonation is DmtA1 from bacteria (*Streptomyces youssoufiensis* OUC68199).[81] DmtA1 and MacJ share 51%/19% sequence similarity/identity (AA), but are located on separate branches in the phylogenetic tree (Fig. 4).

5 Meroterpenoid cyclases in fungal PK-DT pathways

5.1 The GGPP-utilizing cyclases OlcD (deoxyoxalicine B), Cle7 (chevalone E), and Sre3 (sartorypyrone D)

The largest group of discovered fungal PK-T is derived from the C_{15}-precursor FPP and thus, these compounds can be categorized as polyketide sesquiterpenoid hybrids (PK-ST). Apart from this group, several polyketide diterpenoids (PK-DT) derived from the C_{20}-congener GGPP are known from Nature.[1–3]

The first elucidated PK-DT biosynthesis was the deoxyoxalicine A pathway from *Penicillium canescens* ATCC 10419, responsible for the formation of the antiinsectant deoxyoxalicine A (**61**)[60–62] (Scheme 8A). The gene cluster harbors highly homologous genes to the pyripyropene A (**1**) cluster and the same non-terpenoid building block HPPO (**10**) is employed (Scheme 1). However, instead of an FPP-selective prenyl transfer a geranylgeranylation catalyzed by OlcH occurs leading to geranylgeranyl-HPPO (**62**) and subsequent (*S*)-selective epoxidation generates (14*S*)-epoxygeranylgeranyl-HPPO (**63**). The gene cluster for **61** also contains an additional GGPP synthase (OlcC) proposed to facilitate sufficient production of the precursor metabolite GGPP, as deletion led to a strongly reduced production of **61**. The Pyr4-like cyclase OlcD subsequently catalyzes conversion of the PK-DT precursor **63** *via* proposed intermediate **64** to predecaturin E (**65**) from an all-chair substrate conformation. The polyene cyclization is aborted after tricyclic ring formation and terminated by deprotonation of intermediary cation **64** (Scheme 8A). The function of OlcD was shown by gene deletion in the natural producer and isolation of accumulating pathway intermediates.[60]

Apart from OlcD, two other meroterpenoid cyclases in PK-DT biosynthetic pathways have been identified, namely Cle7 and Sre3 towards chevalone E (**66**) from *Aspergillus versicolor* 0312 and sartorypyrone A (**67**) from *Aspergillus felis* 0260 (Scheme 8B).[63] Both

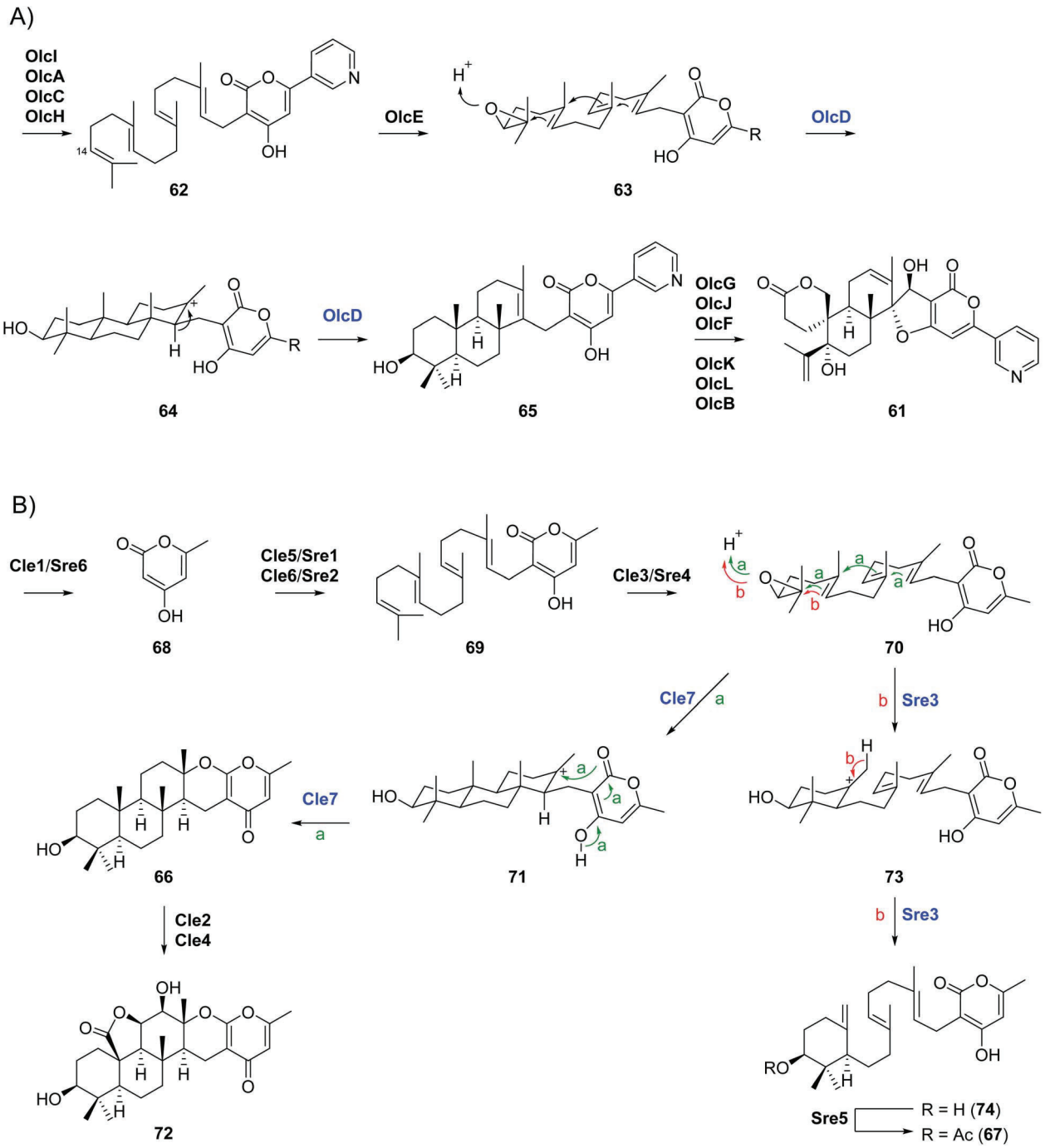

Scheme 8 (A) Pathway towards deoxyoxalicine (**61**) and detailed depiction of meroterpenoid cyclase reaction catalyzed by OlcD. (B) Pathways towards chevalone E (**66**) and sartorypyrone D (**67**) and detailed depiction of meroterpenoid cyclase reactions catalyzed by Cle7 and Sre3.

pathways employ the methyl α-pyrone triacetic acid lactone (TAL, **68**) as the polyketide unit, derived from the PKSs Cle1 and Sre6 in the respective cluster. Both clusters also contain an additional GGPP synthase (Cle6, Sre2), a GGPP-selective prenyltransferase (Cle5, Sre1), and a designated flavin-dependent monooxygenase (Cle3, Sre4) generating (14*S*)-epoxygeranylgeranyl-TAL (**70**).

The branching of the pathways is marked by the action of the respective terpene cyclase. Cle7 converts **70** into chevalone E (**66**) and the stereochemical outcome of the reaction implies an all-chair substrate conformation similar to OlcD catalysis.[60] However, the Cle7-mediated cyclization yields a pentacyclic 6–6–6–6–6 ring system product (**66**) instead of the early abortion product **64** observed for OlcD. Sre3 on the other hand catalyzes only one cyclization to intermediary cation **73** and the reaction is terminated by deprotonation to form sartorypyrone D (**74**) (Scheme 8B).[63]

The three enzymes OlcD, Cle7 and Sre3 share 71–74%/36–44% sequence similarity/identity (AA) and form a specific clade in the phylogenetic tree (Fig. 4). This is interesting to note, since

these enzymes share the same or similar substrates, yet catalyze differing degrees of polyene cyclization. How the enzymes can achieve these distinct reactions and which catalytic residues are responsible to distinguish between early *vs.* late cyclization termination is not known.

5.2 The GGPP-utilizing cyclase SubB and homologs towards decalin diterpenoid pyrones (subglutinol A and higginsianin A)

A second group of fungal PK-DT cyclases was discovered in six pathways towards decalin-containing diterpenoid pyrones, namely the Sub (*Metarhizium robertsii* ARSEF 23), Dpfg (*Fusarium graminearum* 50218), Dpmp (*Macrophomina phaseolina* NBRC7317), Dpch (*Colletotrichum higginsianum* MAFF305635), Dpas (*Arthrinium sacchari*), and Dpma (*Metarhizium anisopliae* E6) pathway.[64,65] Each biosynthetic gene cluster contains the conserved core genes for generation of the polyketide α-pyrone **75** (*subA*/*dpxxA*), GGPP (*subD*/*dpxxD*), their assembly (*subC*/*dpxxC*), and the subsequent activation by an FAD-dependent epoxidase (*subE*/*dpxxE*) to yield the hybrid (10*S*)-epoxy intermediate **77** (Scheme 9). Notably, the epoxidase does not act on the terminal double bond like OlcE, Cle3 and Sre4 (Scheme 8), but instead introduces the epoxide functionality in the C10–C11 position from the 10*Si*,11*Re*-face. All six homologous terpene cyclases (86–91%/58–78% sequence similarity/identity (AA)) are able to convert precursor **77** into the prenyl decalin scaffold **78**. The mechanism can be envisioned from a chair–chair conformation from which after epoxide protonation two ring closing steps occur and the cascade reaction is terminated by deprotonation to form an exomethylene group (Scheme 9).

The pathways diverge after this common intermediate. The Sub, Dpas and Dpma pathway contain only one additional FAD-dependent dehydrogenase (SubF, DpasF, DpmaF) and produce immunusuppressive subglutinol A (**5**).[17 20] The Dpch pathway contains a homologous dehydrogenase (DpchF) producing intermediary **5**, which is further converted to higginsianin A (**79**) by the short chain dehydrogenases DpchG and DpchH (Scheme 9). Compound **79** is the C8 epimer of **5** and does not exhibit

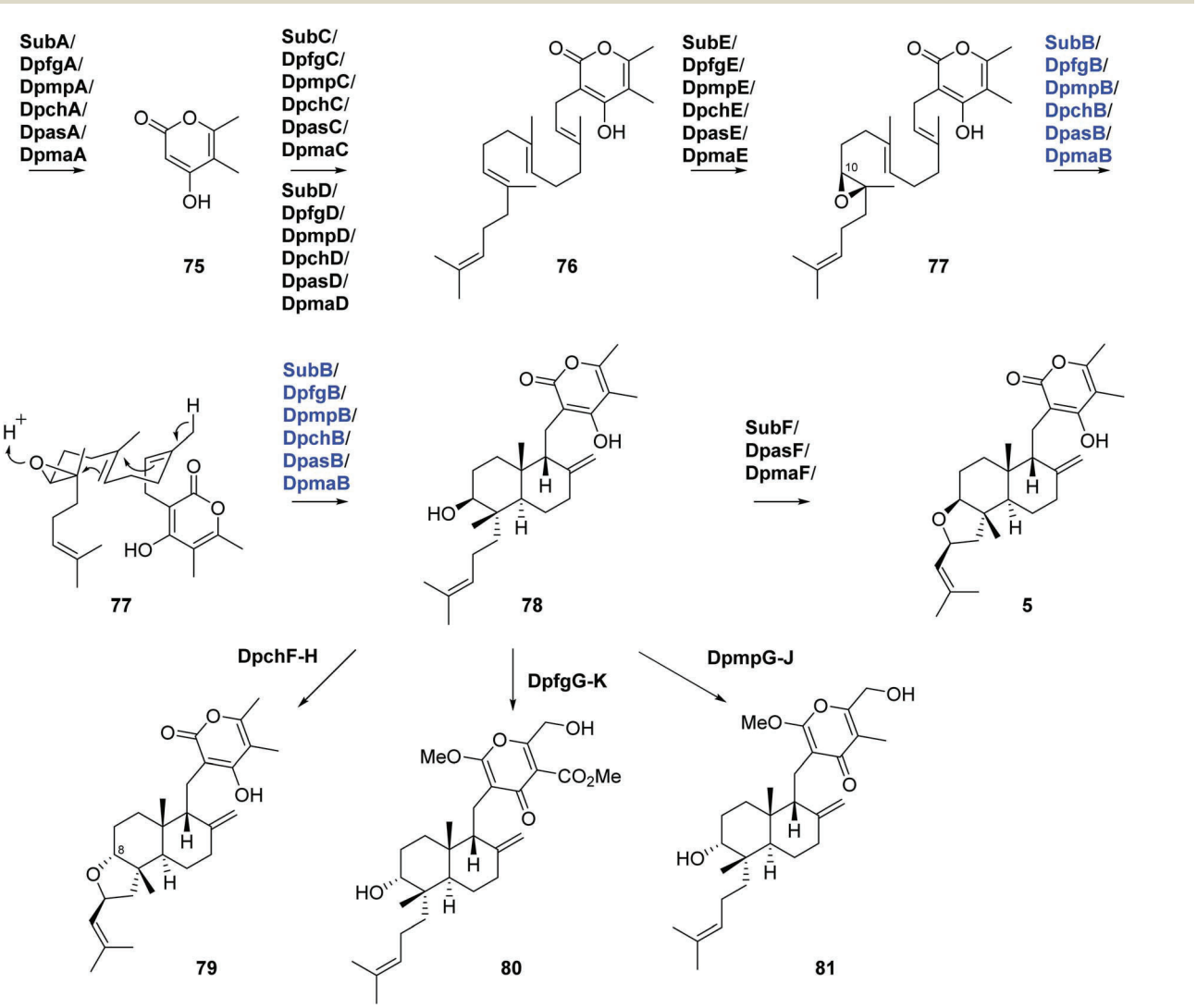

Scheme 9 Pathways towards decalin-containing diterpenoid pyrones and detailed depiction of meroterpenoid cyclase reaction catalyzed by SubB and homolgs.

immunosuppressive activity but antiproliferative effects in Hs683 glioma cancer cells.[93] The pathways Dpfg and Dpmp on the other hand lack a SubF-like dehydrogenase, but contain homologous proteins for the C8-selective hydroxyl group inversion (DpfgG, DpmpG, DpfgH, DpmpH). Additionally, a methyl transferase (DpfgI, DpmpI) and a P450 monooxygenase (DpfgJ, DpmpJ) are encoded in both clusters and the Dpfg pathway contains an additional methyltransferase (DpfgK). Whereas heterologous expression of the combined genes of the Dpf pathway led to the isolation of **80**, the Dpm pathway yielded **81**. Meroterpenoid **80** exhibits cytotoxic and antiproliferative effects on cancer stem-like cells and **81** was found to inhibit amyloid Aβ 42 aggregation, linked to the pathogenesis of Alzheimer's disease.[65]

By combinatorial biosynthetic strategies, the authors additionally accessed eleven novel compounds with differing biological activities such as cell cytotoxicity against cancer cell lines through mitochondrial complex III inhibition, antiproliferative activity against tumor cells (cancer stem-like cells), anti-HIV and antiinsectant properties.[65] These findings are an impressive example for the highly varying bioactivities generated by only small changes in the molecular scaffolds of natural products and underline the great potential of meroterpenoid pathways for engineering efforts.

5.3 The atypical lanosterol synthase-like meroterpenoid cyclase AtnI/NtnI (arthripenoids)

In genome mining efforts for the discovery of novel PK-DT natural products two homologous gene clusters (*atn* and *ntn*) in two phylogenetically distinct fungi (*Arthrinium* sp. NF2194 and *Nectria* sp. Z14-w) were identified.[66] Heterologous gene expression led to the isolation of arthripenoids like arthripenoid C (**82**) for which immunosuppressive properties were determined (Scheme 10).[66]

Both gene clusters contain two PKSs, the highly reducing PKS AtnH/NtnH and the non-reducing PKS AtnG/NtnG which together with the oxidoreductase AtnJ/NtnJ generate the non-terpenoid building block **83**. Subsequently, the FPP-utilizing prenyltransferase AtnF/NtnF yields the farnesylated intermediate **84**. The pathway product arthripenoid C (**82**) indicates that the putative terpene cyclase substrate undergoes epoxidation twice in the biosynthetic pathway. The authors identified two oxidoreductases (AtnK/NtnK and AtnA/NtnA) involved in the suggested sequential epoxidation of **84** to bisepoxide **85** by gene deletion experiments. Additionally, a novel terpene cyclase (AtnI/NtnI) responsible for the formation of **86** was identified. However, whether AtnI/NtnI really converts bisepoxide **85** or a two-step process consisting of C6–C7-epoxidation/cyclization, followed by C10–C11-epoxidation/cyclization occurs could not be clarified as deletion of AtnK/NtnK was unsuccessful and no *in vitro* assays were performed. Such two-step processes are known from indole diterpene pathways and were shown by *in vitro* reactions with synthetic substrates for PaxB/PaxM in the paxilline pathway (for detailed discussion see chapter 6.1).[67] Intriguingly, AtnI/NtnI shows no homology to Pyr4-like cyclases and lacks conserved motifs known for this enzyme family. Instead, AtnI/NtnI exhibits 82–83%/56–59% sequence similarity/identity (AA) to fungal 2,3-oxidosqualene-lanosterol cyclases (Fig. 4).[66] So far, NtnI and AtnI are the only lanosterol synthase-like cyclases identified from fungal meroterpenoid pathways.

6 Meroterpenoid cyclases in fungal ID-DT pathways

6.1 Clustered ID-DT cyclases – PaxB (paxilline) and NodB (nodulisporic acid F)

Several reported fungal indole diterpene (ID-DT) biosynthetic pathways contain Pyr4-like meroterpenoid cyclases and the first

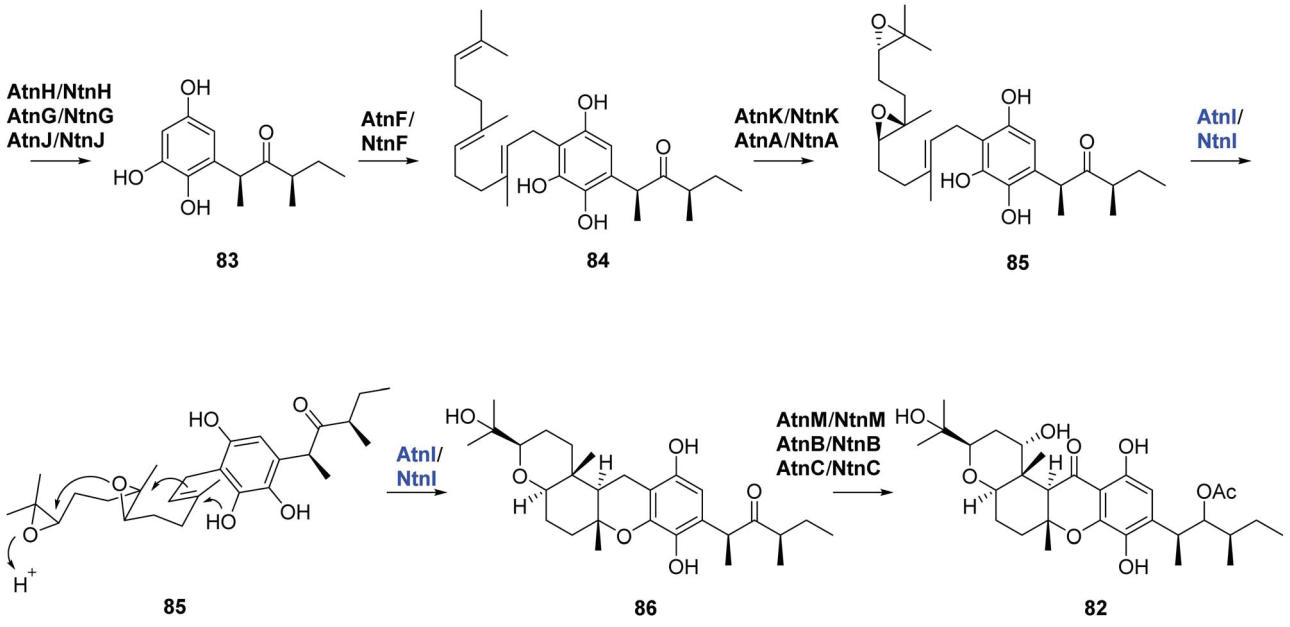

Scheme 10 Pathways towards arthripenoid C and detailed depiction of meroterpenoid cyclase reaction catalyzed by AtnI and NtnI.

characterized example was PaxB from the pathway towards paxilline (**87**) in *Penicillium paxilli* (Scheme 11A).[67] Paxilline and related compounds are tremorgenic compounds that potently inhibit smooth muscle high-conductance calcium-activated potassium channels.[68,69] The paxilline pathway has analogies to the Atn/Ntn pathway since two rounds of epoxidation and cyclization occur. After geranylgeranylation of 1-(3-indoyl) glycerol-3-phosphate (**88**) by PaxC to **89**, the epoxidase PaxM installs an epoxide function in the C10–C11 position of the geranylgeranyl chain to yield **90**. The Pyr4-like cyclase PaxB then catalyzes a sophisticated multistep cyclization reaction. After epoxide opening, the resulting tertiary cation is attacked by the C6–C7 double bond leading to intermediary cation **91**. A second cyclization process by anti-Markovnikov addition to the C2-C3 double bond yields **92** which upon Wagner–Meerwein rearrangement and terminating intramolecular cation quenching yields emindole SB (**94**). A second round of epoxidation by PaxM generates intermediate **95** which is again accepted by PaxB and cyclized to paspaline (**96**). The iterative use of PaxB and PaxM was shown by *in vivo* and *in vitro* experiments with synthetic substrates (Scheme 11A).[67] Several homologous enzymes to PaxB have been reported in ID-DT biosynthetic pathways towards aflatreme (AtmB), lolitreme (LtmB), terpendole E (TerB), penitremane (PenB), or janithremane (JanB).[94 97] These enzymes also catalyze formation of paspaline (**96**) from **90**, but the pathways differ in downstream tailoring enzymes yielding distinct products.

Another recently characterized Pyr4-like cyclase involved in indole diterpenoid biosynthetic pathways is NodB from the pathway towards nodulisporic acid F (**97**) from the filamentous fungus *Hypoxylon pulicicidum* (formerly *Nodulisporium* sp.) (Scheme 11B).[70] Compound **97** and derivatives exhibit highly potent insecticidal activity against blood-feeding arthropods but lack tremorgenic properties associated with the paspaline-derived indole diterpenoids. NodB is able to selectively transform **90**, derived from the action of the transferase NodC and

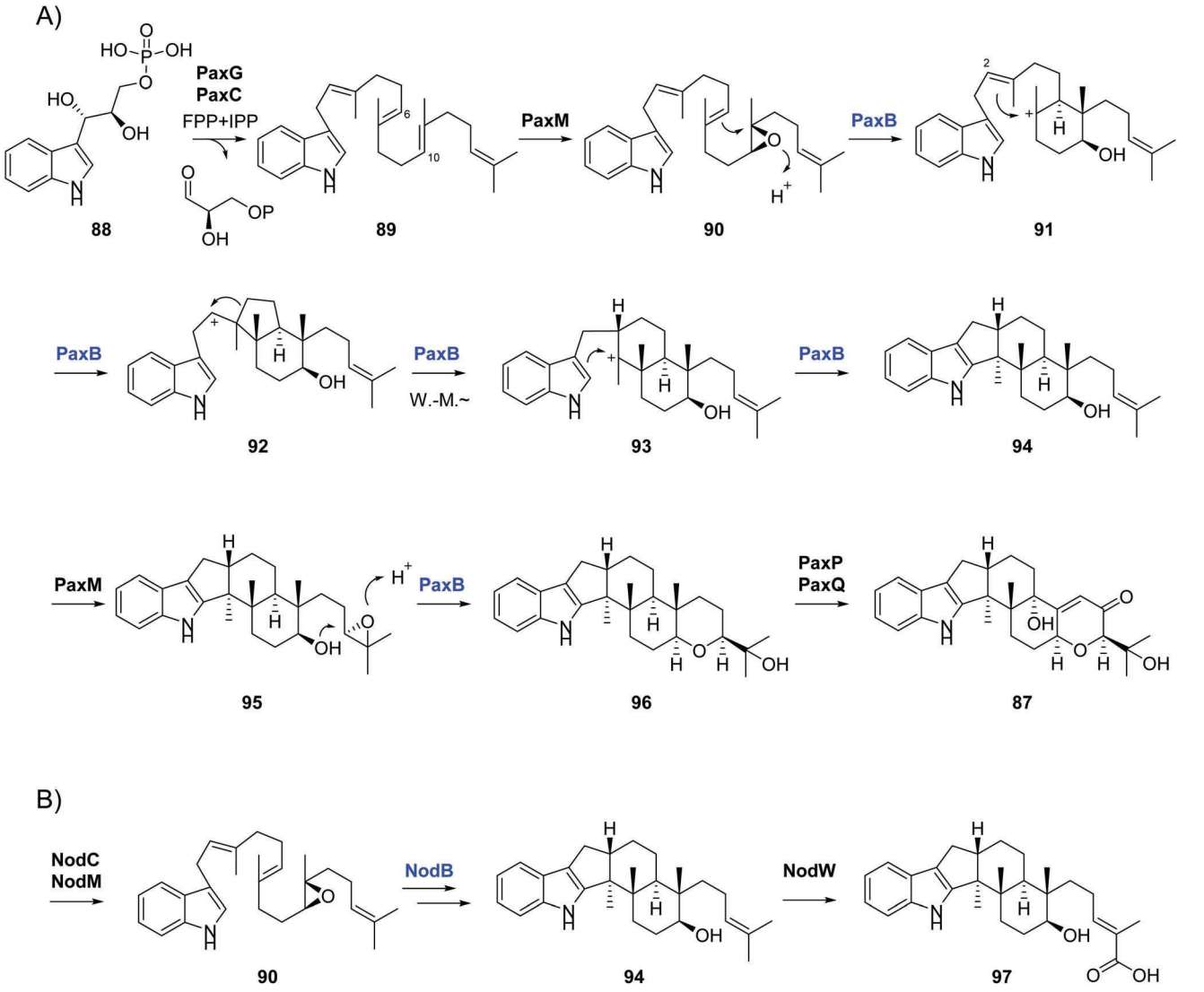

Scheme 11 (A) Pathways towards paxilline (**87**) and detailed depiction of meroterpenoid cyclase reaction catalyzed by PaxB. (B) Pathways towards nodulisporic acid F (**97**) and detailed depiction of meroterpenoid cyclase reaction catalyzed by NodB.

epoxidase NodM into emindole SB (**94**). Distinct to the reaction of PaxB in tandem with the epoxidase PaxM, **94** is not further processed to the paspaline scaffold by NodB and NodM, but subsequently transformed into nodulisporic acid F (**97**) by the P450 monooxygenase NodW.[70]

The paspaline (**96**)-yielding ID-DT cyclases (PaxB, AtmB, LtmB, TerB, PenB, JanB) form a specific clade in the phylogenetic analysis together with emindole SB (**94**)-producing enzyme NodB (Fig. 4).

6.2 Unclustered ID-DT cyclases – AtS2B, AtS5B1, and AfB (emindoles and aflavinines)

Furthermore, three unclustered ID-DT cyclases have been reported from *Aspergillus flavus* (AtS2B, AtS5B1) and *Aspergillus tubingensis* (AfB).[72] Their function was elucidated by phylogenetic considerations to predict their possible substrates and subsequent co-expression in engineered *S. cerevisiae* with suitable substrate-providing enzymes from the aflatrem cluster (AtmG, AtmC, AtmM). The results revealed that all three enzymes can utilize the AtmB/PaxB substrate **90** but differ significantly with respect to their product specificity (Scheme 12A–C).

AtS5B1 shares the early cyclization phase with PaxB, transforming **90** into intermediary cation **93** (Scheme 12A). However, instead of subsequent bond formation to the indole moiety, a 1,2-methyl migration occurs followed by deprotonation to yield intermediate **98**. After a second round of epoxidation by AtmM, AtS5B1 catalyzes formation of the final emindole type product **99**.

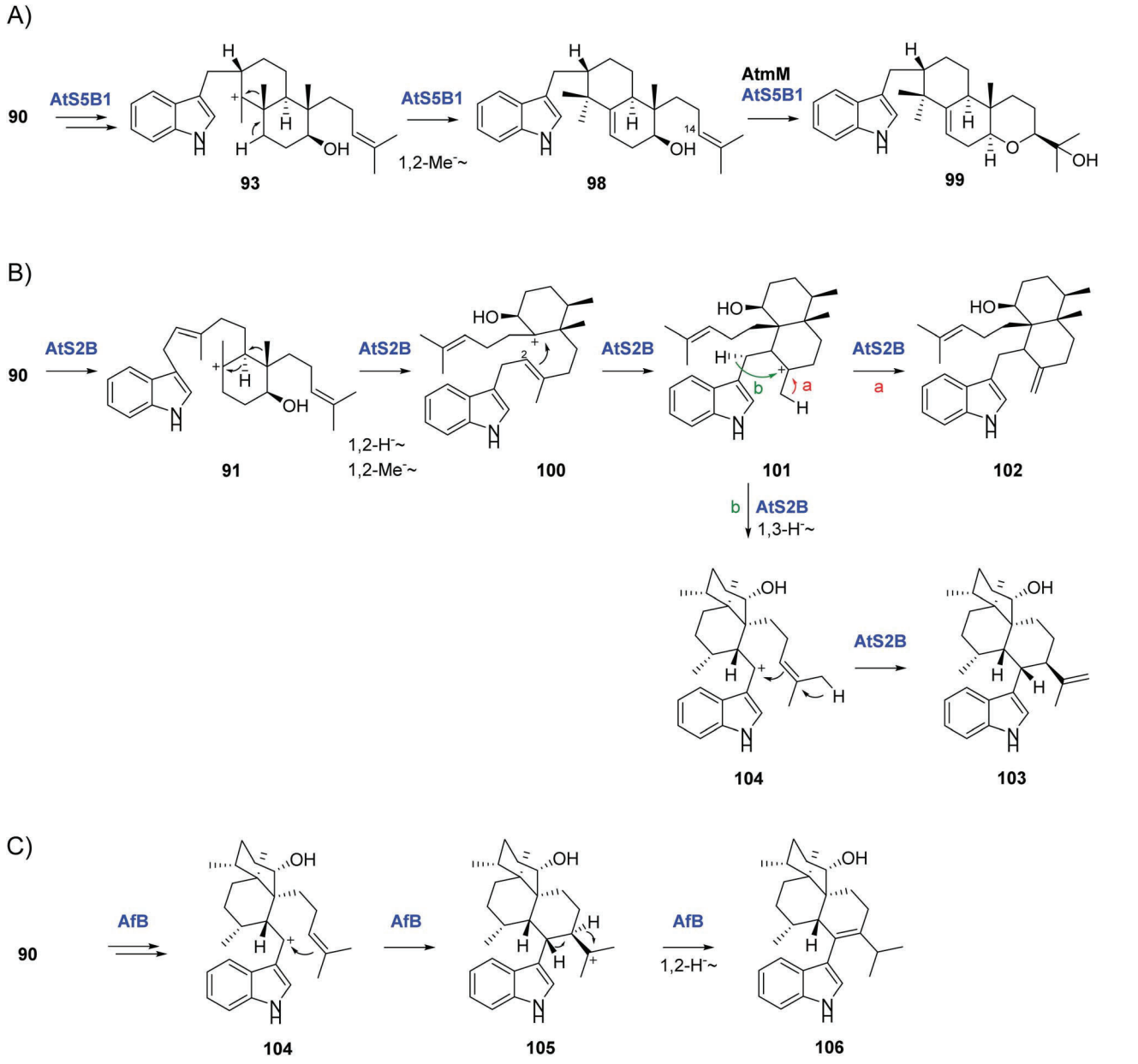

Scheme 12 Reactions of unclustered meroterpenoid cyclases (A) AtS5B1; (B) AtS2B and (C) AfB.

AtS2B on the other hand converts **90** into **91** like PaxB and differs in subsequent cyclization steps (Scheme 12B). Instead of direct formation of a second ring by anti-Markovnikov addition to the C2–C3 double bond, a 1,2-hydride shift, followed by a 1,2 methyl migration occurs to yield tertiary cation **100**. This cation is then attack by the C2–C3 π-bond to give **101**. In the final cyclization phase, AtS2B exhibits promiscuous activity and the two main products anominine (**102**) and 10,23-dihydro-24,25-dehydroaflavinine (**103**) are generated. Whereas anominine (**102**) is formed by a direct terminating deprotonation (path a), formation of **103** can be explained by a preceeding 1,3-hydride shift yielding **104** from which a third 6-membered ring is generated by attack of the C14–C15 double bond, followed by terminating deprotonation (path b, Scheme 12B).

AfB shares 85%/58% sequence similarity/identity (AA) to AtS2B, which is resembled in their shared production of intermediary cation **104** from **90** (Scheme 12C). However, both enzymes differ in the late stage of the cyclization cascade. After the third ring formation to intermediate **105**, AfB catalyzes a 1,2-hydride shift followed by terminating deprotonation yielding the final product aflavinine (**106**). Notably, ID-DT cyclases seem to exhibit a certain degree of product promiscuity, as AfB was found to generate several minor side products including **102** and the AtS5B1 expressing strain accumulated small amounts of **94**, **96**, and **98**.[72]

Whereas AtS2B and AfB form a new clade in the phylogenetic analysis and appear to be only distantly related to other ID-DT cyclases, AtS5B1 is found on the same branch as the PaxB group of enzymes (Fig. 4). These findings are consistent with the observed differences in product specificity as AtS5B1 catalyzes anti-Markovnikov-addition in the early cyclization phase towards an emindole type product (**99**), whereas AtS2B and AfB omit this reaction pathway and form the aflavinine scaffolds (**102**, **103**, **106**).

7 Summary and future perspective

In summary, fungal meroterpenoid cyclases are versatile catalysts with impressive abilities for structural diversification in meroterpenoid biosynthetic pathways. The discovery of the first member of this family of non-canonical, membrane-integrated proteins Pyr4 from the pyripyropene pathway allowed for the identification and characterization of several new enzymes with unique and distinct activities.

These advances paved the way to exploit and harvest the potential of these biocatalysts for second generation natural product discovery by pathway engineering efforts like combinatorial biosynthesis.[98] The detailed understanding of the sophisticated enzyme mechanisms and how they are controlled by the acting cyclase still awaits to be elucidated and protein structural data is highly desired. Furthermore, it will set the stage for rational protein engineering efforts to further expand the chemical space of fungal meroterpenoids and will allow for the discovery of valuable novel compounds.

8 Conflicts of interest

There are no conflicts to declare.

9 Acknowledgements

We thank a Grant-in-Aid for Scientific Research from the Ministry of Education, Culture, Sports, Science and Technology, Japan (JSPS KAKENHI Grant Number JP16H06443 and JP20H00490 to I. A.) and the Deutsche Forschungsgemeinschaft (DFG BA 6870/1-1) for a postdoctoral research fellowship to L. B.

10 Notes and references

1 R. Geris and T. J. Simpson, *Nat. Prod. Rep.*, 2009, **26**, 1063–1094.
2 Y. Matsuda and I. Abe, *Nat. Prod. Rep.*, 2016, **33**, 26–53.
3 Y. Matsuda and I. Abe, *Comprehensive Natural Products III: Chemistry and Biology*, Elsevier, 2020, vol. 1, Chapter 14, pp. 445–478.
4 S. Omura, H. Tomoda, Y. K. Kim and H. Nishida, *J. Antibiot.*, 1993, **46**, 1168–1169.
5 H. Tomoda, Y. K. Kim, H. Nishida, R. Masuma and S. Omura, *J. Antibiot.*, 1994, **47**, 148–153.
6 A. Das, M. A. Davis, H. Tomoda, S. Ômura and L. L. Rudel, *J. Biol. Chem.*, 2008, **283**, 10453–10460.
7 R. Horikoshi, K. Goto, M. Mitomi, K. Oyama, T. Sunazuka and S. Omura, *J. Antibiot.*, 2017, **70**, 272–276.
8 K. Goto, R. Horikoshi, M. Mitomi, K. Oyama, T. Hirose, T. Sunazuka and S. Omura, *J. Antibiot.*, 2018, **71**, 785–797.
9 K. Goto, R. Horikoshi, S. Nakamura, M. Mitomi, K. Oyama, T. Hirose, T. Sunazuka and S. Omura, *J. Pestic. Sci.*, 2019, **44**, 255–263.
10 K. Goto, R. Horikoshi, M. Mitomi, K. Oyama, T. Hirose, T. Sunazuka and S. Omura, *J. Antibiot.*, 2019, **72**, 661–681.
11 R. Kandasamy, D. London, L. Stam, W. von Deyn, X. Zhao, V. L. Salgado and A. Nesterov, *Insect Biochem. Mol. Biol.*, 2017, **84**, 32–39.
12 C. Dieleman, T. Knieriem, M. Krapp, P. C. Kierkus, W. Xu and K. Benton, Composition Containing a Pyripyropene Insecticide and a Base, WO 2012/035010 A1, 2012.
13 T. J. Franklin and J. M. Cook, *Biochem. J.*, 1969, **113**, 515–524.
14 R. Bentley, *Chem. Rev.*, 2000, **100**, 3801–3825.
15 M. D. Sintchak, M. A. Fleming, O. Futer, S. A. Raybuck, S. P. Chambers, P. R. Caron, M. A. Murcko and K. P. Wilson, *Cell*, 1996, **85**, 921–930.
16 P. C. L. Ferreira, F. V. Thiesen, A. G. Pereira, A. R. Zimmer and P. E. Fröehlich, *Clin. Transplant.*, 2020, **34**, e13997.
17 J. C. Lee, E. Lobkovsky, N. B. Pliam, G. Strobel and J. Clardy, *J. Org. Chem.*, 1995, **60**, 7076–7077.
18 G. A. Strobel and N. B. Pliam, Immunosuppressant secondary metabolite diterpenes and method of production using a fungal organism, *US Pat.* 5648376A, 1997.
19 H. Kim, J. B. Baker, S. U. Lee, Y. Park, K. L. Bolduc, H. B. Park, M. G. Dickens, D. S. Lee, Y. Kim, S. H. Kim and J. Hong, *J. Am. Chem. Soc.*, 2009, **131**, 3192–3194.
20 R. Lin, H. Kim, J. Hong and Q. J. Li, *ACS Med. Chem. Lett.*, 2014, **5**, 485–490.
21 M. Cueto, J. B. MacMillan, P. R. Jensen and W. Fenical, *Phytochemistry*, 2006, **67**, 1826–1831.

22 S. Omura, J. Inokoshi, R. Uchida, K. Shiomi, R. Masuma, T. Kawakubo, H. Tanaka, Y. Iwai, S. Kosemura and S. Yamamura, *J. Antibiot.*, 1996, **49**, 414–417.
23 R. Uchida, K. Shiomi, J. Inokoshi, T. Sunazuka, H. Tanaka, Y. Iwai, H. Takayanagi and S. Omura, *J. Antibiot.*, 1996, **49**, 418–424.
24 D. W. Christianson, *Chem. Rev.*, 2017, **117**, 11570–11648.
25 J. S. Dickschat, *Nat. Prod. Rep.*, 2016, **33**, 87–110.
26 K. U. Wendt, G. E. Schulz, E. J. Corey and D. R. Liu, *Angew. Chem., Int. Ed.*, 2000, **39**, 2812–2833.
27 T. Itoh, K. Tokunaga, Y. Matsuda, I. Fujii, I. Abe, Y. Ebizuka and T. Kushiro, *Nat. Chem.*, 2010, **2**, 858–864.
28 H. C. Lo, R. Entwistle, C. J. Guo, M. Ahuja, E. Szewczyk, J. H. Hung, Y. M. Chiang, B. R. Oakley and C. C. C. Wang, *J. Am. Chem. Soc.*, 2012, **134**, 4709–4720.
29 Y. Matsuda, T. Awakawa, T. Wakimoto and I. Abe, *J. Am. Chem. Soc.*, 2013, **135**, 10962–10965.
30 C. J. Guo, B. P. Knox, Y. M. Chiang, H. C. Lo, J. F. Sanchez, K. H. Lee, B. R. Oakley, K. S. Bruno and C. C. C. Wang, *Org. Lett.*, 2012, **14**, 5684–5687.
31 T. Itoh, K. Tokunaga, E. K. Radhakrishnan, I. Fujii, I. Abe, Y. Ebizuka and T. Kushiro, *ChemBioChem*, 2012, **13**, 1132–1135.
32 Y. Matsuda, T. Awakawa, T. Itoh, T. Wakimoto, T. Kushiro, I. Fujii, Y. Ebizuka and I. Abe, *ChemBioChem*, 2012, **13**, 1738–1741.
33 Y. Matsuda, T. Iwabuchi, T. Wakimoto, T. Awakawa and I. Abe, *J. Am. Chem. Soc.*, 2015, **137**, 3393–3401.
34 J. P. Springer, J. W. Dorner, R. J. Cole and R. H. Cox, *J. Org. Chem.*, 1979, **44**, 4852–4854.
35 Y. Matsuda, T. Awakawa and I. Abe, *Tetrahedron*, 2013, **69**, 8199–8204.
36 Y. Matsuda, Z. Quan, T. Mitsuhashi, C. Li and I. Abe, *Org. Lett.*, 2016, **18**, 296–299.
37 J. F. Rojas-Aedo, C. Gil-Durán, A. Del-Cid, N. Valdés, P. Álamos, I. Vaca, R. O. García-Rico, G. Levicán, M. Tello and R. Chávez, *Front. Microbiol.*, 2017, **8**, 813.
38 Y. Matsuda, T. Iwabuchi, T. Fujimoto, T. Awakawa, Y. Nakashima, T. Mori, H. Zhang, F. Hayashi and I. Abe, *J. Am. Chem. Soc.*, 2016, **138**, 12671–12677.
39 D. B. Stierle, A. A. Stierle, J. D. Hobbs, J. Stokken and J. Clardy, *Org. Lett.*, 2004, **6**, 1049–1052.
40 D. B. Stierle, A. A. Stierle and B. Patacini, *J. Nat. Prod.*, 2007, **70**, 1820–1823.
41 I. Kjærbølling, T. C. Vesth, J. C. Frisvad, J. L. Nybo, S. Theobald, A. Kuo, P. Bowyer, Y. Matsuda, S. Mondo, E. K. Lyhne, M. E. Kogle, A. Clum, A. Lipzen, A. Salamov, C. Y. Ngan, C. Daum, J. Chiniquy, K. Barry, K. LaButti, S. Haridas, B. A. Simmons, J. K. Magnuson, U. H. Mortensen, T. O. Larsen, I. V. Grigoriev, S. E. Baker and M. R. Andersen, *Proc. Natl. Acad. Sci. U. S. A.*, 2018, **115**, E753–E761.
42 Y. Matsuda, T. Bai, C. B. W. Phippen, C. S. Nødvig, I. Kjærbølling, T. C. Vesth, M. R. Andersen, U. H. Mortensen, C. H. Gotfredsen, I. Abe and T. O. Larsen, *Nat. Commun.*, 2018, **9**, 2587.
43 Y. Matsuda, T. Wakimoto, T. Mori, T. Awakawa and I. Abe, *J. Am. Chem. Soc.*, 2014, **136**, 15326–15336.
44 Y. Nakashima, T. Mitsuhashi, Y. Matsuda, M. Senda, H. Sato, M. Yamazaki, M. Uchiyama, T. Senda and I. Abe, *J. Am. Chem. Soc.*, 2018, **140**, 9743–9750.
45 T. Bai, Y. Matsuda, H. Tao, T. Mori, Y. Zhang and I. Abe, *Org. Lett.*, 2020, **22**, 4311–4315.
46 Q. Li, C. Chen, L. Cheng, M. Wei, C. Dai, Y. He, J. Gong, R. Zhu, X. N. Li, J. Liu, J. Wang, H. Zhu and Y. Zhang, *J. Org. Chem.*, 2019, **84**, 1534–1541.
47 T. Bai, Z. Quan, R. Zhai, T. Awakawa, Y. Matsuda and I. Abe, *Org. Lett.*, 2018, **20**, 7504–7508.
48 H. Yamazaki, W. Nakayama, O. Takahashi, R. Kirikoshi, Y. Izumikawa, K. Iwasaki, K. Toraiwa, K. Ukai, H. Rotinsulu, D. S. Wewengkang, D. A. Sumilat, R. E. P. Mangindaan and M. Namikoshi, *Bioorg. Med. Chem. Lett.*, 2015, **25**, 3087–3090.
49 Y. Araki, T. Awakawa, M. Matsuzaki, R. Cho, Y. Matsuda, S. Hoshino, Y. Shinohara, M. Yamamoto, Y. Kido, D. K. Inaoka, K. Nagamune, K. Ito, I. Abe and K. Kita, *Proc. Natl. Acad. Sci. U. S. A.*, 2019, **116**, 8269–8274.
50 Z. Quan, T. Awakawa, D. Wang, Y. Hu and I. Abe, *Org. Lett.*, 2019, **21**, 2330–2334.
51 G. Tamura, S. Suzuki, A. Takatsuki, K. Ando and K. Arima, *J. Antibiot.*, 1968, **21**, 539–544.
52 S. H. Lee, C. H. Kwak, S. K. Lee, S. H. Ha, J. Park, T. W. Chung, K. T. Ha, S. J. Suh, Y. C. Chang, H. W. Chang, Y. C. Lee, B. S. Kang, J. Magae and C. H. Kim, *J. Cell. Biochem.*, 2016, **117**, 978–987.
53 J. H. Kang, J. K. Kim, W. H. Park, K. K. Park, T. S. Lee, J. Magae, H. Nakajima, C. H. Kim and Y. C. Chang, *J. Cell. Biochem.*, 2007, **102**, 506–514.
54 Y. Miyazaki, D. K. Inaoka, T. Shiba, H. Saimoto, T. Sakura, E. Amalia, Y. Kido, C. Sakai, M. Nakamura, A. L. Moore, S. Harada and K. Kita, *Front. Pharmacol.*, 2018, **9**, 997.
55 H. Sasaki, T. Hosokawa, M. Sawada and K. Ando, *J. Antibiot.*, 1973, **26**, 676–680.
56 N. Minagawa, Y. Yabu, K. Kita, K. Nagai, N. Ohta, K. Meguro, S. Sakajo and A. Yoshimoto, *Mol. Biochem. Parasitol.*, 1997, **84**, 271–280.
57 D. K. Holm, L. M. Petersen, A. Klitgaard, P. B. Knudsen, Z. D. Jarczynska, K. F. Nielsen, C. H. Gotfredsen, T. O. Larsen and U. H. Mortensen, *Chem. Biol.*, 2014, **21**, 519–529.
58 M. C. Tang, X. Cui, X. He, Z. Ding, T. Zhu, Y. Tang and D. Li, *Org. Lett.*, 2017, **19**, 5376–5379.
59 H. Fujimoto, E. Nakamura, Y. P. Kim, E. Okuyama, M. Ishibashi and T. Sassa, *J. Nat. Prod.*, 2001, **64**, 1234–1237.
60 J. Yaegashi, J. Romsdahl, Y. M. Chiang and C. C. C. Wang, *Chem. Sci.*, 2015, **6**, 6537–6544.
61 C. Li, J. B. Gloer, D. T. Wicklow and P. F. Dowd, *J. Nat. Prod.*, 2005, **68**, 319–322.
62 Y. Zhang, C. Li, D. C. Swenson, J. B. Gloer, D. T. Wicklow and P. F. Dowd, *Org. Lett.*, 2003, **5**, 773–776.
63 W. G. Wang, L. Q. Du, S. L. Sheng, A. Li, Y. P. Li, G. G. Cheng, G. P. Li, G. Sun, Q. F. Hu and Y. Matsuda, *Org. Chem. Front.*, 2019, **6**, 571–578.

64 H. Kato, Y. Tsunematsu, T. Yamamoto, T. Namiki, S. Kishimoto, H. Noguchi and K. Watanabe, *J. Antibiot.*, 2016, **69**, 561–566.
65 K. Tsukada, S. Shinki, A. Kaneko, K. Murakami, K. Irie, M. Murai, H. Miyoshi, S. Dan, K. Kawaji, H. Hayashi, E. N. Kodama, A. Hori, E. Salim, T. Kuraishi, N. Hirata, Y. Kanda and T. Asai, *Nat. Commun.*, 2020, **11**, 1830.
66 X. Zhang, T. T. Wang, Q. L. Xu, Y. Xiong, L. Zhang, H. Han, K. Xu, W. J. Guo, Q. Xu, R. X. Tan and H. M. Ge, *Angew. Chem., Int. Ed.*, 2018, **57**, 8184–8188.
67 K. Tagami, C. Liu, A. Minami, M. Noike, T. Isaka, S. Fueki, Y. Shichijo, H. Toshima, K. Gomi, T. Dairi and H. Oikawa, *J. Am. Chem. Soc.*, 2013, **135**, 1260–1263.
68 H. G. Knaus, O. B. McManus, S. H. Lee, W. A. Schmalhofer, M. Garcia-Calvo, L. M. H. Helms, M. Sanchez, K. Giangiacomo, J. P. Reuben, A. B. Smith, G. J. Kaczorowski and M. L. Garcia, *Biochemistry*, 1994, **33**, 5819–5828.
69 C. O. Miles, A. L. Wilkins, R. T. Gallagher, A. D. Hawkes, S. C. Munday and N. R. Towers, *J. Agric. Food Chem.*, 1992, **40**, 234–238.
70 K. C. Van de Bittner, M. J. Nicholson, L. Y. Bustamante, S. A. Kessans, A. Ram, C. J. van Dolleweerd, B. Scott and E. J. Parker, *J. Am. Chem. Soc.*, 2018, **140**, 582–585.
71 J. G. Ondeyka, G. L. Helms, O. D. Hensens, M. A. Goetz, D. L. Zink, A. Tsipouras, W. L. Shoop, L. Slayton, A. W. Dombrowski, J. D. Polishook, D. A. Ostlind, N. N. Tsou, R. G. Ball and S. B. Singh, *J. Am. Chem. Soc.*, 1997, **119**, 8809–8816.
72 M. C. Tang, H. C. Lin, D. Li, Y. Zou, J. Li, W. Xu, R. A. Cacho, M. E. Hillenmeyer, N. K. Garg and Y. Tang, *J. Am. Chem. Soc.*, 2015, **137**, 13724–13727.
73 J. B. Gloer, B. L. Rinderknecht, D. T. Wicklow and P. F. Dowd, *J. Org. Chem.*, 1989, **54**, 2530–2532.
74 H. J. Wang, J. B. Gloer, D. T. Wicklow and P. F. Dowd, *Appl. Environ. Microbiol.*, 1995, **61**, 4429–4435.
75 R. T. Gallagher, T. McCabe, K. Hirotsu, J. Clardy, J. Nicholson and B. J. Wilson, *Tetrahedron Lett.*, 1980, **21**, 243–246.
76 J. B. Gloer, M. R. TePaske, J. S. Sima, D. T. Wicklow and P. F. Dowd, *J. Org. Chem.*, 1988, **53**, 5457–5460.
77 H. Li, Q. Zhang, S. Li, Y. Zhu, G. Zhang, H. Zhang, X. Tian, S. Zhang, J. Ju and C. Zhang, *J. Am. Chem. Soc.*, 2012, **134**, 8996–9005.
78 Z. Xu, M. Baunach, L. Ding and C. Hertweck, *Angew. Chem., Int. Ed.*, 2012, **51**, 10293–10297.
79 H. Li, Y. Sun, Q. Zhang, Y. Zhu, S. M. Li, A. Li and C. Zhang, *Org. Lett.*, 2015, **17**, 306–309.
80 L. Ding, J. Münch, H. Goerls, A. Maier, H. H. Fiebig, W. H. Lin and C. Hertweck, *Bioorg. Med. Chem. Lett.*, 2010, **20**, 6685–6687.
81 T. Yao, J. Liu, Z. Liu, T. Li, H. Li, Q. Che, T. Zhu, D. Li, Q. Gu and W. Li, *Nat. Commun.*, 2018, **9**, 4091.
82 Q. Che, T. Zhu, X. Qi, A. Mándi, T. Kurtán, X. Mo, J. Li, Q. Gu and D. Li, *Org. Lett.*, 2012, **14**, 3438–3441.
83 U. Omasits, C. H. Ahrens, S. Müller and B. Wollscheid, *Bioinformatics*, 2014, **30**, 884–886.
84 H. C. Lin, Y. H. Chooi, S. Dhingra, W. Xu, A. M. Calvo and Y. Tang, *J. Am. Chem. Soc.*, 2013, **135**, 4616–4619.
85 R. Schor, C. Schotte, D. Wibberg, J. Kalinowski and R. J. Cox, *Nat. Commun.*, 2018, **9**, 1963.
86 Y. H. Chooi, R. Cacho and Y. Tang, *Chem. Biol.*, 2010, **17**, 483–494.
87 J. D. Rudolf and C. Y. Chang, *Nat. Prod. Rep.*, 2020, **37**, 425–463.
88 L. A. M. Murray, S. M. K. McKinnie, B. S. Moore and J. H. George, *Nat. Prod. Rep.*, 2020, DOI: 10.1039/D0NP00018C.
89 K. Poralla, A. Hewelt, G. D. Prestwich, I. Abe, I. Reipen and G. Sprenger, *Trends Biochem. Sci.*, 1994, **19**, 157–158.
90 T. S. Lin, Y. M. Chiang and C. C. C. Wang, *Org. Lett.*, 2016, **18**, 1366–1369.
91 X. M. Mao, Z. J. Zhan, M. N. Grayson, M. C. Tang, W. Xu, Y. Q. Li, W. B. Yin, H. C. Lin, Y. H. Chooi, K. N. Houk and Y. Tang, *J. Am. Chem. Soc.*, 2015, **137**, 11904–11907.
92 T. S. Bugni, D. Abbanat, V. S. Bernan, W. M. Maiese, M. Greenstein, R. M. Van Wagoner and C. M. Ireland, *J. Org. Chem.*, 2000, **65**, 7195–7200.
93 A. Cimmino, V. Mathieu, M. Masi, R. Baroncelli, A. Boari, G. Pescitelli, M. Ferderin, R. Lisy, M. Evidente, A. Tuzi, M. C. Zonno, A. Kornienko, R. Kiss and A. Evidente, *J. Nat. Prod.*, 2016, **79**, 116–125.
94 T. Motoyama, T. Hayashi, H. Hirota, M. Ueki and H. Osada, *Chem. Biol.*, 2012, **19**, 1611–1619.
95 M. J. Nicholson, C. J. Eaton, C. Stärkel, B. A. Tapper, M. P. Cox and B. Scott, *Toxins*, 2015, **7**, 2701–2722.
96 M. J. Nicholson, A. Koulman, B. J. Monahan, B. L. Pritchard, G. A. Payne and B. Scott, *Appl. Environ. Microbiol.*, 2009, **75**, 7469–7481.
97 C. A. Young, M. K. Bryant, M. J. Christensen, B. A. Tapper, G. T. Bryan and B. Scott, *Mol. Genet. Genomics*, 2005, **274**, 13–29.
98 T. Mitsuhashi, L. Barra, Z. Powers, V. Kojasoy, A. Cheng, F. Yang, Y. Taniguchi, T. Kikuchi, M. Fujita, D. J. Tantillo, J. A. Porco Jr and I. Abe, *Angew. Chem., Int. Ed.*, 2020, DOI: 10.1002/anie.202011171.